Turowski, J., Cook, K. (2017): Field techniques for measuring bedrock erosion and denudation. - *Earth Surface Processes and Landforms*, *42*, 1, pp. 109—127.

DOI: http://doi.org/10.1002/esp.4007

EARTH SURFACE PROCESSES AND LANDFORMS
Earth Surf. Process. Landforms **42**, 109–127 (2017)

Published online 31 August 2016 in Wiley Online Library
(wileyonlinelibrary.com) DOI: 10.1002/esp.4007

State of Science

Field techniques for measuring bedrock erosion and denudation

Jens M. Turowski* and Kristen L. Cook
GFZ German Research Centre for Geosciences, Potsdam, Germany

Received 11 December 2015; Revised 11 July 2016; Accepted 19 July 2016

*Correspondence to: Jens M. Turowski, GFZ German Research Centre for Geosciences, Section 5.1, Telegrafenberg, 14473 Potsdam, Germany. E-mail: turowski@gfz-potsdam.de

ESPL
Earth Surface Processes and Landforms

ABSTRACT: Bedrock erosion rates in natural landscapes are usually slow, of the order of millimeters per year or less, and sophisticated techniques have been developed to measure them. Different techniques have proved to be valuable depending on the spatial and temporal scale on which information is needed, on the environment and on the scientific question that is asked. Here, we give an overview of the various methods that have been developed. We introduce their working principles and outline their advantages and disadvantages. Further, we provide comprehensive references to relevant literature, both on the methods and on scientific examples of their application. © 2016 The Authors. Earth Surface Processes and Landforms published by John Wiley & Sons Ltd.

KEYWORDS: bedrock erosion; erosion; denudation; field methods; review

Introduction

The shape of the Earth's surface results from a competition between uplift and erosion. Erosion is driven by a number of physical, chemical, and biological processes dependent on local conditions such as climate, substrate, and tectonics. To further our understanding of how these processes work, we rely on precise rate measurements in the field or in the laboratory. Erosion can occur rapidly (e.g. Lamb and Fonstad, 2010; Cook *et al.*, 2013), but more often it is a slow and rare process (e.g. Molnar *et al.*, 2006; Koppes and Montgomery, 2009). Therefore, accurate measurements of erosion rates are challenging, and a large amount of creativity has gone into developing suitable methods. In this contribution, we review field methods to measure erosion and denudation rates. It is not the aim of the paper to give an exhaustive description of each method with all the scientific and technical details needed to apply it; rather, we aim to provide a survey of available methods, highlighting their scope of application and relative merits, in order to provide the reader with an overview as to which methods are suitable for his or her research.

Erosion rate (E) is defined as the ratio between a change in surface position with respect to a benchmark Δh, and a change in time Δt:

$$E = \frac{\Delta h}{\Delta t} \tag{1}$$

<NI>Direct techniques for measuring erosion rates rely on measuring both Δh and Δt for the same setting. Bedrock erosion rates are generally slow, typically below 1mm/yr (cf. Koppes and Montgomery, 2009), and it is rare that erosion rates are so rapid that they can be readily observed. Thus, field techniques can be generally grouped in two classes. In the first class, here termed *dating methods*, erosion rates are determined over long timescales. In this case, Δh can be obtained from geological markers, such as the elevation of strath terraces above the current river channel, and the challenge lies in the accurate dating of the markers or deposits. The overall error in the rate measurement is dominated by the error in the dating method. In the second class, here termed *survey methods*, the shape of a surface of interest is surveyed at two or more points in time, typically after several months to years. The change in time Δt can be measured to high accuracy with a clock and the challenge in this case is the high-resolution survey of the bedrock topography. Here, the overall error in the rate measurements is dominated by the error resulting from the comparison of height at different points in time. In addition to these two classes of methods, bedrock erosion rates can be obtained indirectly by measuring or estimating the material discharged from a certain area and upscaling the findings to long timescales.

This review is consequently structured in four parts. First, after introducing some general definitions and nomenclature, we review dating methods that can be applied to bedrock surfaces. Second, we review methods for topographic measurements that can be used to obtain bedrock wear. In addition, we describe methods that have so far been used only for measuring erosion of loose sediment, because they can serve as inspiration for new bedrock erosion measurement techniques. In both these two parts, the physical or chemical background of the methods is described, equipment and field requirements are outlined, key publications are pointed out, and illustrative

examples for each method are discussed, as far as they are available. Third, we review indirect methods of measurement. Fourth, we discuss some general pitfalls and give tips for erosion measurements. Although the review focusses on measurement methods for bedrock erosion, many of the methods can be also employed in other environments.

Measurement Methods

Some nomenclature

For a definition of the term erosion in geomorphic usage, we quote the words of Gilbert (1877):

> All indurated rocks and most earths are bound together by a force of cohesion which must be overcome before they can be divided and removed. The natural processes by which the division and removal are accomplished make up erosion.

According to Gilbert (1877), the erosion process can be divided in general into weathering, transportation and corrasion, and thus can include physical, chemical and biological processes. We define *denudation* as the loss of mass from a landscape through both solids and solutes (cf. Anderson and Anderson, 2010), which thus includes all erosion processes. Methods of measuring erosion often yield either local erosion rates, which can be process-specific, or landscape-wide denudation rates that integrate over all processes acting in a landscape. The terms erosion and denudation can also be distinguished from a method-specific view. While erosion is measured locally by assessing how much material is lost at a point (inside perspective – eroded material moves away from the observer), denudation can be measured by quantifying how much material is discharged from a certain area (outside perspective – eroded material moves towards the observer). The term *exhumation* means the upwards displacement of rocks relative to the Earth's surface. It relates to long timescales and is often used in tectonic contexts.

Any measurement is associated with an error, and reporting a measured data value without quantifying its error renders the information meaningless. In general, we can discriminate between *systematic errors* and *random errors*. Random errors are related to the noise that affects any measurement. They can be detected by systematically repeating the measurement, and their overall impact can be reduced by averaging over many individual data points. In contrast, systematic errors are related to the construction of the measurement method and the necessary devices, and to the way the operator uses them. They typically arise because the actual experimental arrangement is different from that assumed in theory. Systematic errors are hard to detect and easy to miss. A *statistic* is a parameter that is completely determined by the data. A *bias* arises if a statistic is obtained in such a way that it is systematically different from the corresponding parameter in the population. The term bias includes systematic errors, but also incorrect use of devices, statistics, and methods by an operator, or misinterpretation of results. *Accuracy* means the degree of closeness of a measurement to the actual true value of what is measured. In contrast, the term *precision* relates to the reproducibility of a result under the same conditions, using the same method of measurement. Thus, accuracy relates to systematic errors, while precision relates to random errors. A measurement method can be accurate, but not precise, precise, but not accurate, both, or neither. It is of course desirable, if it is both precise and accurate. In contrast, *tolerance* is an engineering term that means the permissible limit of the quantity in question in the application in question. The differences between precision, accuracy, and tolerance may be important, as different communities may refer to different concepts when reporting measurement errors or technical standards of devices. When different quantities are combined to yield a final result, like in measurements of erosion rate, which is the ratio of a distance and a time (Equation 1), errors of the individual quantities can be combined using error propagation theory (e.g. Ku, 1966). For a more elaborate treatment of the topic of errors, the reader is directed to textbooks on experimental method, such as Squires (1998).

Erosion rates are measured in units of distance per time. Typically, bedrock erosion and denudation rates are given in either of the equivalent forms of millimeters per year, meters per thousand years, or kilometers per million years, depending on the timescale of consideration. Fischer (1969) introduced the Bubnoff as a unit of geological erosion, which is equivalent to one meter per million years, but the use of this unit never caught on (see Berg and Gangi, 1971).

Dating methods

Dating methods make use of marker surfaces or deposits, such as fluvial terraces, paleosols, paleo surfaces or relict landscapes (e.g. Burbank *et al.*, 1996; Barke and Lamb, 2006; Prince and Spotila, 2013), moraines, fluvial or lacustrine deposits (e.g. Pratt-Sitaula *et al.*, 2007; Craddock *et al.*, 2010), sculpted fluvial surfaces (e.g. Schaller *et al.*, 2005; Reusser *et al.*, 2006), pediments, caves (e.g. Polyak *et al.*, 2008; Häuselmann *et al.*, 2007; Stock *et al.*, 2005), lava flows (e.g. Pederson *et al.*, 2002; Karlstrom *et al.*, 2007) and tephras (e.g. Dethier, 2001), or travertine (e.g. Pederson *et al.*, 2002; Zentmyer *et al.*, 2008), that record the former elevation or position of a feature of interest. The difference between the position of the marker and the present position of the feature of interest can be observed, and the erosion rate can be determined by measuring the age of the marker. The most common application of this method is the dating of fluvial terraces or sculpted fluvial surfaces to constrain rates of river incision. In some cases, the age of the marker surface can be known exactly, such as surfaces created by historical volcanic eruptions (e.g. Whipple *et al.*, 2000) and man-made surfaces (e.g. Johnson *et al.*, 2010).

There are a number of techniques that can be used to date geomorphic surfaces or marker deposits, for each of which extensive literature exists. Because excellent descriptions are available, we will briefly mention the most common techniques and point the reader towards existing reviews or exemplary case studies for each method.

Cosmogenic exposure and burial dating

Cosmogenic exposure dating can be used to date both bedrock and alluvial surfaces, and relies on the production of cosmogenic isotopes in material at or near the Earth's surface (Gosse and Phillips, 2001). In nuclear reactions, secondary cosmic rays produce cosmogenic nuclides in minerals located in the top few meters of soil or bedrock (Lal and Peters, 1967). The rate of production is depth-dependent, and if this dependence is known, the concentration of cosmogenic nuclides in a grain can give information about the time this grain has spent near or at the surface. For simple exposure dating one assumes that erosion of the surface is negligible. If this assumption is valid, and the surface has not been disturbed in any other way, the method can yield the exposure time to cosmogenic rays of any surface containing suitable material. Several cosmogenic

nuclides have been used in geomorphic work (Lal, 1991), but ^{10}Be has proved to be an ideal isotope in surface dating and erosion (Granger and Riebe, 2014). Practically, beryllium-10 (^{10}Be) is produced only by cosmogenic rays from the parent isotope oxygen-16 (^{16}O), which is abundant in the most common mineral at the Earth's surface, quartz. Thus, ^{10}Be dating techniques can be applied in a wide range of environments. Furthermore, ^{10}Be is not only produced from oxygen in quartz, but also in the atmosphere. This so-called meteoric ^{10}Be then rains onto the Earth's surface, where it is adsorbed by soil and fine-grained sediments and can be used to determine soil and sediment ages and residence times (Willenbring and von Blanckenburg, 2010b). Cosmogenic nuclides have been used to date fluvial terraces (e.g. Burbank *et al.*, 1996), relict fluvial surfaces (e.g. Schaller *et al.*, 2005), large landslides (e.g. Ivy-Ochs *et al.*, 2009), and bedrock eroded by a glacier (e.g. Nishiizumi *et al.*, 1989). Care needs to be taken to interpret the data using knowledge of the geomorphic processes that contributed to forming the studied surface.

Using the same method under slightly different theoretical assumptions, erosion rates can be measured directly. In this case, one assumes that the surface is not stable, but has been eroding at a constant rate over the temporal scale of the measurement. The concentration of the cosmogenic nuclide in a sample then reflects the amount of time the sample took to travel from several meters depth to the surface and therefore the erosion rate (Lal, 1991). This allows for point measurements of soil production and erosion (e.g. Heimsath *et al.*, 1997), and of bedrock erosion rates directly from eroding surfaces such as bedrock river channels (e.g. Hancock *et al.*, 1998), tors (e.g. Hancock and Kirwan, 2007), and bedrock outcrops (e.g. Portenga and Bierman, 2011). If multiple cosmogenic isotopes are used, for instance ^{10}Be and aluminum-26 (^{26}Al), it may be possible to obtain constraints on both the exposure and erosion of the surface (Lal, 1991; Bierman *et al.*, 1999). A detailed exposition of the theory and practice of cosmogenic exposure dating and erosion measurement using ^{10}Be, including examples, has been given by Granger and Riebe (2014).

Similarly, in *cosmogenic burial dating*, one takes advantage of the decay of two cosmogenic isotopes, ^{10}Be and ^{26}Al, both of which form in quartz. When the mineral is exposed to cosmogenic rays, these isotopes are produced at a constant ratio, but they decay at different rates. Thus, their relative abundance evolves through time after production has ceased and can be used to determine the timing of burial, that is, of the onset of shielding from cosmogenic rays by overlying material (e.g. Granger and Muzikar, 2001; Repka *et al.*, 1997).

Dating marker deposits

A number of methods exist to date sedimentary deposits, depending on the material available, and the history and age of the deposit. Many of these methods are well established and excellent review papers or textbooks are available. Thus, we will not give a lot of details here, but refer to the specialist literature.

Due to ionizing radiation, electrons within a mineral can get trapped on higher energy levels than their base state. When stimulated by light, they may fall back into their base state and emit a photon in the process. *Optically stimulated luminescence* (OSL) dating exploits this effect in the dating of quartz and potassium feldspar grains (Wallinga, 2002). By measuring the amount of luminescence upon optical stimulation, the amount of time since the material has been bleached by exposure to sunlight can be obtained. This provides constraints on the timing of deposition and burial of fine grained (silt to fine sand) sediment that has remained undisturbed since deposition (e.g. Harkins *et al.*, 2007; Yanites *et al.*, 2010). OSL dating can be used for a wide range of deposit ages, from ~50 to 300 000 years. Reviews of OSL dating have been given by Wallinga (2002) and Madsen and Murray (2009).

Radiocarbon, or carbon-14 (^{14}C), is produced by cosmic rays in the atmosphere and is incorporated in organic matter through respiration. Because the proportion of ^{14}C in the organic material depends on the time since the death of the organism, this method provides a maximum constraint on the age of the deposit containing datable organic matter (Libby, 1955; Lowe, 1991; Harkins *et al.*, 2007). Thus, ^{14}C has a half-life of 5730 years, thus restricting the use of the method to deposits younger than about 50 000 years (Walker, 2005).

U-series dating of pedogenic carbonate provides minimum ages for soils and gravel deposits, as it dates post-deposition carbonate accumulation (Schwarcz, 1989; Sharp *et al.*, 2003; Candy *et al.*, 2004). U-series dating takes advantage of the difference in solubility between uranium and thorium in soil waters, which are generally enriched in uranium and highly depleted in thorium. Carbonate precipitated from these waters therefore contains negligible initial thorium, so as uranium-234 (^{234}U) decays to thorium-230 (^{230}Th), the age of the carbonate is tracked by the relative abundance of the two elements. Because the nuclides of U-Th decay chain are all radioactive, the system eventually reaches secular equilibrium and the maximum ages that can be measured are ~500 kyr. Similarly, U-series dating can also be applied to travertine and may provide information about the elevation of the water table (Polyak *et al.*, 2008) or the age of alluvial deposits (Pederson *et al.*, 2002).

Other possible techniques to constrain timing of deposition include *magnetostratigraphy,* which is based on the tendency of fine-grained sediment to preserve the polarity of the Earth's magnetic field at the time of deposition (Sasowsky *et al.*, 1995; Li *et al.*, 1997; Stock *et al.*, 2005; Craddock *et al.*, 2012), and *biostratigraphy*, which relies on the presence of appropriate fossils within the deposit, the age of which is known from other deposits (Schildgen *et al.*, 2012). In *dendrochronological methods*, a date can be established and possibly tied to an environmental change by counting back the annual tree rings corresponding to individual years. Likewise, the year of death of wood can be found by comparing to a reference chronology of living trees nearby, as ring width is related to environmental conditions. Soil erosion rates have been determined by dating of the time when roots were first exposed (e.g. Carrara and Carroll, 1979). This technique has been reviewed by Stoffel *et al.* (2013), and may be viable in special circumstances for bedrock erosion.

Uncertainties in dating methods

There are two primary sources of error related to dating methods. First, there are the uncertainties of the measurements themselves. These are specific to each dating method and include both the analytical uncertainties and those associated with the particular assumptions required by a given method. The uncertainty in the amount of erosion (Δh; the distances between marker features; see Equation 1) is included in this category. In some cases this can be significant, for example when a fluvial incision rate estimate requires determining the depth to bedrock in a river with thick and variable alluvial cover (cf. Karlstrom *et al.*, 2007).

The second source of error is related to the relationship between the measured ages and the histories of the marker features. In the case of fluvial terraces, different techniques date different events in the life of a terrace, such as pre-deposition death of organic material (^{14}C), deposition (magnetostratigraphy, biostratigraphy), burial (luminescence, cosmogenic burial dating), abandonment (cosmogenic exposure ages), and post-deposition

carbonate accumulation (U-series dating). Each of these has different implications for the meaning of the measured age and its relationship to the onset of incision. Different methods also have different susceptibility to later modification, and events such as reworking, erosion, and later deposition on marker features can significantly alter the meaning of a measured age. It is also important to be aware that these methods are measuring average rates for processes that may be quite unsteady. This can lead to biases depending on the measurement period (cf., Finnegan *et al.*, 2014), and misinterpretation of typical rates of erosion, particularly for processes or locations where short-lived transient erosion events dominate (cf. The Sadler effect, later).

Survey methods

Survey methods rely on the repeated topographic measurement of a surface at two different times. The two measurements are then compared and erosion or deposition can be calculated from the differences. In general, for survey methods it is easy to accurately measure Δt, and the challenge lies in obtaining Δh from the topographic measurements (cf. Equation 1). There are two main sources of errors. First, the survey method itself is associated with a specific accuracy and precision. Second, it is often challenging to identify benchmark points that are stable over time, that do not affect the outcome of the measurement, and that are common in both measurements. In fact, often the availability of high-quality benchmarks limits the overall accuracy of the method.

In the following, we describe various techniques that have been developed to measure surface changes in the field, moving from simple to more complex methods. Survey methods for the measurement of erosion in loose substrates in general have been reviewed by Gleason (1957), Miller and Leopold (1962), Lawler (1993), and Hudson (1993), who focused on soil and bank erosion, and by Lisle and Eads (1991) and Schuett-Hames *et al.* (1996) in the context of gravel scour in river channels. Reviews of specific methods are pointed out in the relevant sections.

Erosion painting

By applying paint to a surface and checking whether it is still there after an erosive event, one can gain information on the spatial distribution of erosion in the landscape. Dietrich *et al.* (2005) and Surian *et al.* (2009) painted patches of sediment in streams to see whether they were mobilized in floods, and Gill and Lang (1983) applied dots of paint to rock to find suitable locations for more detailed study. Beer *et al.* (2016) compared the patterns of erosion revealed from the removal of paint to those obtained from repeat topographic measurements in a proof-of-concept study and concluded that erosion painting is a cheap and quick technique that can give semi-quantitative information on erosion patterns over potentially large areas. In addition, since the paint's *erodibility*, i.e. the resistance of a material to being eroded, is the same everywhere, with erosion painting one can obtain insight in the spatial variability of the *erosivity*, i.e. the power to erode of the process in question.

Benchmarking

Differences in erodibility, whether they occur naturally or are artificially introduced, are often exploited when measuring erosion. The *benchmarking* family of methods relies on the notion that erosion rates are negligible over the survey period for the part of the surface with low erodibility. Thus, these areas can be used as a stable benchmark, and erosion rates for the part of the surface with high erodibility can be obtained by comparing the different parts of the surface using simple distance measurements. Natural *differences in erodibility* or *shielding* of surfaces have mainly been exploited in erosion measurements of soils and of soft bedrock. An example is the use of pedestal markers such as rocks, shrubs and other plants (Fig. 1A, e.g. Dunne *et al.*, 1978; Vanwalleghem *et al.*, 2010; Lucía *et al.*, 2011). This technique was apparently pioneered by Rapp *et al.* (1972), and today is often used by non-scientists to assess soil erosion rates (e.g. Okoba and Sterk, 2006). Artificial shielding of soils has been done using bottle tops (Gleason, 1957) or coins (Della Seta *et al.*, 2007) pressed into the ground. Artificial shielding of bedrock from erosion has to our knowledge not been used in the field, but shielding plane bedrock surfaces by bolting on a steel plate may be a simple way of creating an artificial benchmark surface. Simple and low cost benchmarks in bedrock surfaces are holes that can easily be drilled into hard bedrock (Hancock *et al.*, 1998). If the depth of the hole is measured before and after an erosive event, the erosion rate of the surrounding surface can be obtained. The disadvantage of this technique is that the holes are difficult to clean of sand, pebbles and other particles that often get lodged in them.

The most common low-cost benchmarking technique consists of the installation of *erosion pins, bolts, stakes,* or *nails* (Figs. 1B and 1C; for simplicity, we use the term bolt hereafter). Bolts are installed in bedrock by either placing them in a borehole, using glue or expansion anchors for fixing them (hard rock), or by driving them in with a hammer (soft rock) such that their orientation is normal to the rock's surface. Bolts are generally manufactured from hard material such as steel; welding rods in particular have proved to be suitable for soil erosion monitoring (Evans, 1967). The bolt thus represents an artificial benchmark with low erodibility (Haigh, 1977). The distance from the bolt head to the eroding surface can be measured before and after erosion events and the difference can be used to calculate erosion rates. The bolt method is preferable to natural benchmarks, as it should be clearly visible when the bolt itself has been eroded, and the measurement can be ignored or corrected in this case. Erosion bolts have been used to assess soil erosion rates at least since the 1950s (Colbert, 1956), and the method was widely used in the 1960s and 1970 (e.g. Leopold *et al.*, 1966; Hadley and Lusby, 1967; Imeson, 1971; Haigh, 1977). A few authors have successfully used the bolt technique to study bedrock erosion, both for soft and hard bedrock (Montgomery, 2004; Stock *et al.*, 2005; Clarke and Rendell, 2006; Johnson *et al.*, 2010).

The erosion bolt method has been modified to obtain additional information, and also to obtain better temporal resolution of erosion rates. Duncan and Ward (1985) added a slider to their bolt, which moved downwards with the eroding surface, but was buried when deposition occurred. By digging out the device after an event, the maximum depth of scour and the subsequent depth of deposition can be obtained. Erlingsson (1991) and Lawler (1991) apparently independently designed an erosion bolt equipped with a series of photovoltaic sensors, dubbed *photo-electronic erosion pin* (PEEP) by the latter. Originally conceived for the monitoring of bank retreat, the device can record both erosion and deposition of material to high temporal and spatial precision, as long as there is external light. The position of the bank can thereby be located in between active and inactive photovoltaic sensors, and the timing of changes can be recorded on a logger. The PEEP has been further developed and used in a number of studies (e.g. Lawler, 1992; Lawler *et al.*, 2001). In order to overcome the limitation to daytime measurements, temperature sensors were included next to the photovoltaic sensors, exploiting the temperature differences between water, air, and soil (Lawler, 2005, 2008).

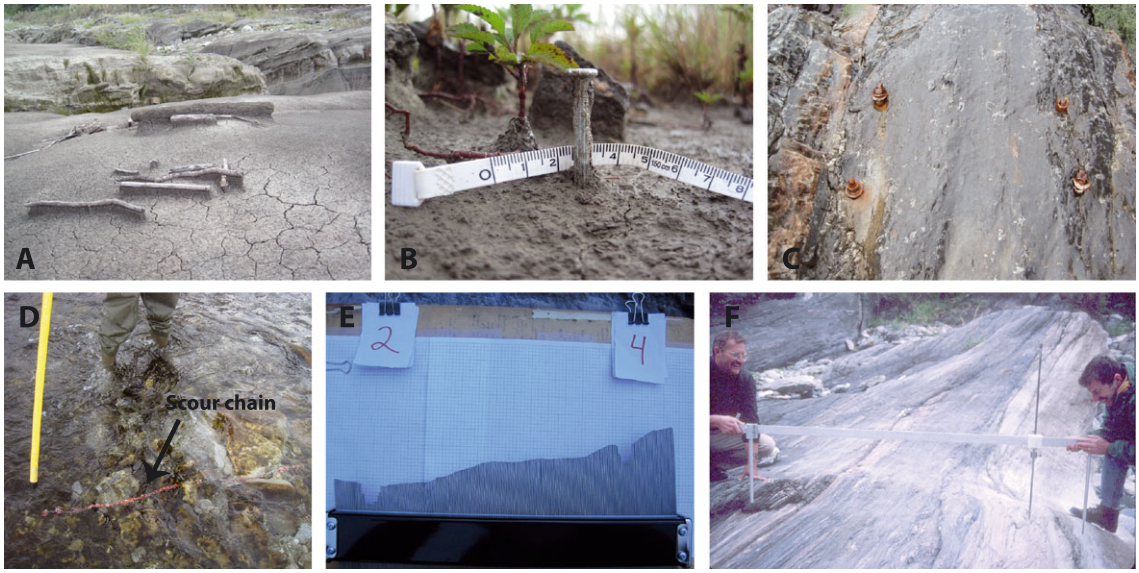

Figure 1. Measuring erosion in the field. (A) Natural shielding of a surface by logs as pedestal markers. (B) An erosion bolt in soft rock, inserted by well-aimed hammer strikes. (C) A set of bolts used as reference points for a profile gauge, localized scour and damage to the bolts illustrate potential pitfalls of erosion bolts. (D) Scour chain (red) in a river channel. (E) A profile gauge with multiple spikes (caterpillar), illustrating the acquisition of data. (F) A profile gauge with a movable engineering gauge for measuring the distance to the rock (photograph courtesy N. Hovius).

The conditions during events that are capable of eroding bedrock are often violent and it seems likely that any devices that stick out from the eroding rock are damaged or destroyed, limiting the application of sophisticated and therefore expensive bolt methods. A related problem common to all artificial benchmark techniques is that the presence of the benchmark may affect the nearby physical processes and thus alter the local erosion rates. For example, bolts protruding into the flow of a channel could alter local flow fields and thus affect local erosion rates. Stock *et al.* (2005) checked with hand-level surveying that this was not the case in their study. But especially in violent turbulent conditions and when erosion is driven by particle impact this effect could significantly bias results. A systematic investigation of this issue has to our knowledge not been published.

Some of these problems can be addressed by using *ecessed benchmarks* (Fig. 2), similar to the target system developed by Wilson *et al.* (2013). Thereby, a screw socket is fixed into a drilled hole such that it is set well below the bedrock surface. In between surveys, the hole is closed with a plug or a glue. When surveying, the hole is opened up, and a target benchmark is inserted in the socket. The distance from the target to the rock surface can then be measured to obtain erosion rates. Alternatively, a point gauging instrument could be placed on the recessed benchmarks (e.g. Hartshorn *et al.*, 2002; see later).

A variant of the erosion bolt method is the *scour chain* (Fig. 1D), where instead of a rigid bolt a flexible chain is used (Colby, 1964; Laronne and Duncan, 1989; Laronne *et al.*, 1994). The scour chain method can also be viewed as a hybrid between a survey method and erosion tracking (see earlier).

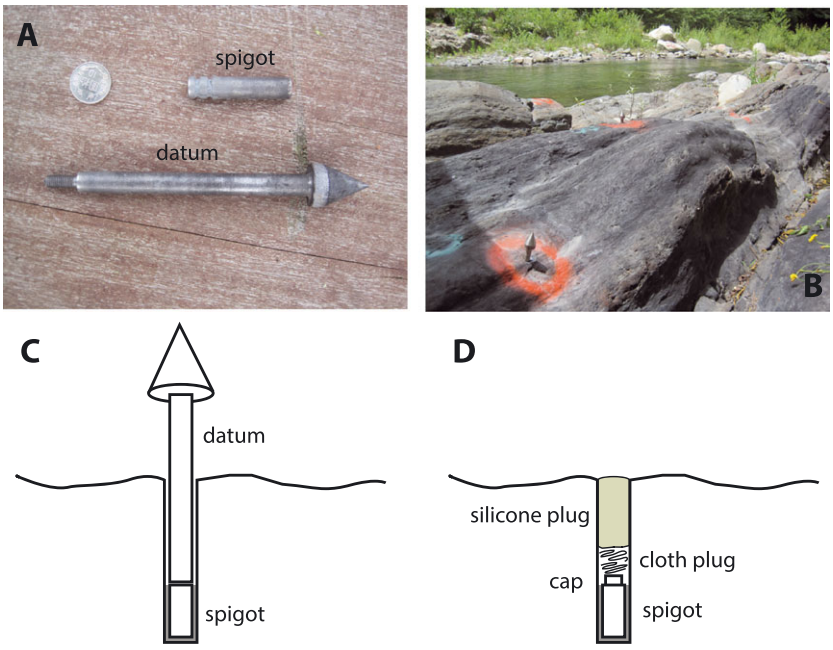

Figure 2. Recessed benchmark, consisting of spigot and datum, shown before installation (A) and in use in the field (B). For installation, the spigot is fixed into a hole drilled into the rock at the site of interest (C). When not in use, the hole is closed with silicon to protect the installation (D). When the benchmark is needed, the hole is opened up again, and the datum is screwed into the spigot.

The advantage of this system is two-fold. First, in loose substrate, one can obtain the maximum scour depth as well as the height of re-deposited sediment. Second, arguably the flow field around the site is less disturbed by the presence of a flexible chain then by a rigid bolt. However, this second aspect has not been systematically studied. For the study of bedrock erosion, scour chains could be fixed into drill holes with an expansion anchor.

Erosion tracking

As *erosion tracking* we classify methods in which a device is eroded in parallel with the surrounding surface, and this erosion is tracked and recorded. The method offers an alternative to erosion bolts and other benchmark methods, since no or only small parts of the instrument protrude into the erosive flow and the erosion process is thus largely undisturbed by the measurement device. However, the erodibility of the device may differ from that of the surrounding area and care needs to be taken when interpreting the data.

One of the earliest erosion tracking devices is the *sliding-bead monitor* used for the study of gravel scour (Nawa and Frissell, 1993). In this technique, a number of beads are threaded onto a cable such that they can slide. The bead cable is placed vertically in the ground, and a few meters of spare cable are left loose. As the ground is eroded, the beads are mobilized and slide along the cable until they hit a stopper at its end. When revisiting the site after an erosion event, the number of beads at the end of the cable can be counted to obtain the erosion depth. The system has been improved by adding a magnetic gate near the end of cable that can be used to record the time of arrival of individual beads (DeVries *et al.*, 2001). Thus, the temporal evolution of scour can be measured. The sliding-bead monitor has not been used to study the erosion of hard bedrock. A problem for its use may be the destructive environment at interesting sites – the cable might be destroyed and eroded beads would in this case not be found after an event. However, simple adaption of the system may make it suitable for the study of bedrock erosion. For example, individual beads could be numbered and marked by different colors, such that the number of missing beads could be inferred from the ones remaining in the hole.

A more sophisticated method, *resistance tracking*, relies on the measurement of resistance changes (Fig. 3). The principle is simple: a thin network of parallel wired resistors is placed normal to the surface in a drill hole in the bedrock. By passing a voltage across the network, the total resistance can be measured. As the surface wears down, individual resistor units are likewise eroded, resulting in stepwise changes of the total resistance, and the timing and magnitude of these changes are logged. Such a system was used by Berger *et al.* (2010, 2011 to measure erosion of loose material by debris flows. A similar device with much higher spatial resolution was developed by Dubille (2009) and Lavé and Dubille (2011) for the monitoring of hard bedrock, and later adapted by Beer *et al.* (2015) and Beer and Turowski (2015). To install the latter instrumentation into the rock, a core with a diameter of 7 to 10 cm and a depth of 40 to 50 cm is taken at the site of interest. Subsequently, the core is shortened to 10–15 cm and lengthwise cut in half. With the resistor network placed in between, the two halves are rejoined together using a glue with low viscosity. Finally, the core is replaced in the field in its original position and fixed with a suitable cement or glue. A logger unit can be placed in the hole underneath. Versions of the system with an additional access hole for the downloading of data or with Bluetooth data transmission have been successfully tested (A. Beer, J. Lavé, personal communication). Recording at frequencies of five minutes gives battery lives of several months to years, and spatial resolutions of 0.05 mm have been achieved.

Point gauging and surveying

Point gauging and *surveying* techniques rely on the availability of fixed benchmarks, on which a precision instrument (e.g. a total station) can be placed (Fig. 4). These benchmarks should not move or erode between survey campaigns. Surveying relies on the measurement of distance and angles between a base station and a target. Modern survey instruments can be very accurate and precise, and with fixed survey points outside the area of interest, high-quality data can be obtained in many field settings. Many excellent text books on classical survey techniques are available (e.g. Anderson and Mikhail, 1998). Surveying can also be done with the global positioning system (GPS), and differential GPS can achieve location accuracies in the centimeter range. Examples of classic surveying in the context of bedrock

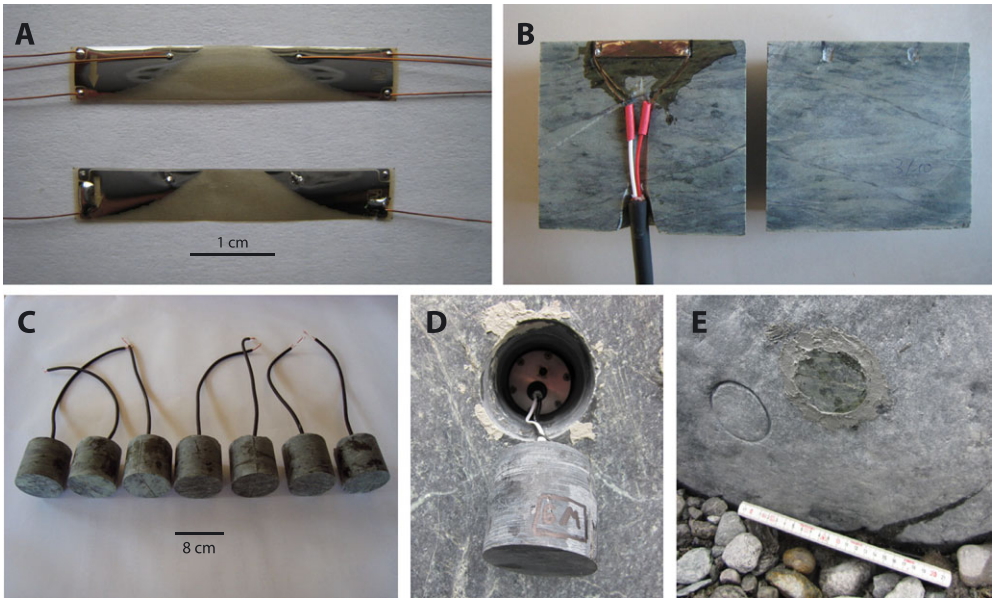

Figure 3. A resistance tracking device. A network of parallel wires, here a modified commercially available crack gauge (A), is glued between the two halves of a core sourced from the rock of interest (B, C). The core is then replaced into its original hole (D, E), with an independent logger unit hidden in the rock underneath it. Photographs A, B, C, D courtesy of A. Beer.

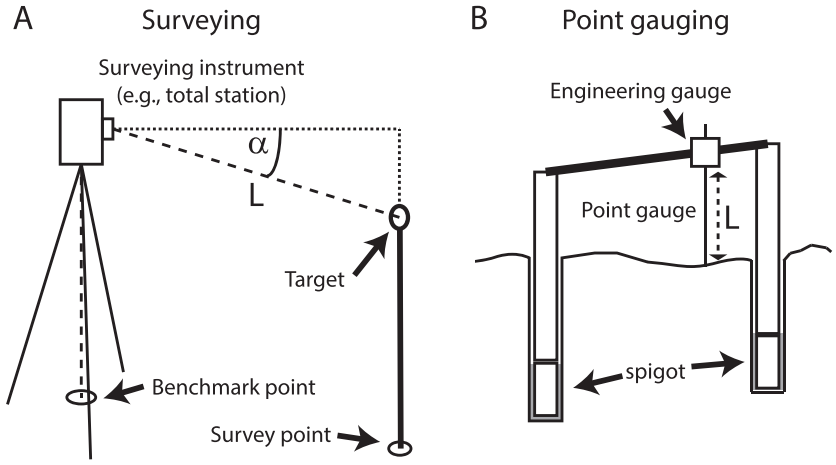

Figure 4. Surveying (A) compared to point gauging (B). Surveying relies on the measurement of angles and distances between a survey instrument located on a fixed benchmark. These measurements are then used to calculate the location of the surveyed points (A). In point gauging one directly measures the distance between the instrument and the surveyed point, while the angles between the instrument and the surveyed point are fixed (B). Since, when point gauging, a single distance value needs to be measured, the potential number of sources of error is minimized in comparison to surveying and very high precision can be achieved.

erosion can be found in the publications of Howard and Kerby (1983), Chatanantavet and Parker (2011) and Turowski *et al.* (2013). A disadvantage of surveying techniques is the need for operators in the field, so data at high temporal resolution during erosive events cannot be taken. Also, the high number of individual measurements that needs to be made (height of instrument, height of target, distance, vertical angle, horizontal angle) leads to a complicated error structure, limiting the overall accuracy that can be achieved. When measurements at very high accuracy and precision are needed, point gauging is a suitable alternative.

Point gauging has a long history in erosion measurements dating back to the 1960s (Hudson, 1964), and if carefully designed and operated, it allows for accuracy and precision that surpass many other available techniques (Spate *et al.*, 1985; Williams *et al.*, 2000; Swantesson *et al.*, 2006). Point gauging instruments have been designed to measure at a point (e.g. High and Hanna, 1970), along a line (e.g. Hartshorn *et al.*, 2002), or distributed over an area (e.g. Stephenson, 1997), but the applied principle is always the same. The measurement is made directly with a physical device, for instance an engineering gauge, which can measure precisely the distance between a point in the instrument and the surface of interest. Fixed benchmarks on the rock surface are necessary to place the device.

Profile or *contour gauges* have long been used in geomorphology (Hudson, 1964). A profile gauge is a linear instrument that either features multiple measurement devices (Fig. 1E; e.g. De Jong, 1992) or a slider holding a single device (Fig. 1F; e.g. Hartshorn *et al.*, 2002). Multiple similar, often independent designs have been described (e.g. McCool *et al.*, 1981; Smart *et al.*, 2004; Kornecki *et al.*, 2008), including ones with semi-automated or automated data acquisition (e.g. Römkens *et al.*, 1986; Hirschi *et al.*, 1987; Khorashahi *et al.*, 1987), and sub-millimeter precision has been achieved. The devices have been used in a number of studies for the measurement of bedrock erosion (Hartshorn *et al.*, 2002; Turowski *et al.*, 2008; Johnson *et al.*, 2010).

The most highly developed and best studied point gauging instrument to date is the micro-erosion meter (MEM) (Fig. 5). Designed by Hanna (1966) and High and Hanna (1970) for the study of erosion of rock shore platforms, the MEM has since been continuously used and developed (Stephenson, 2013). The MEM consists of a precision engineering gauge mounted on a tripod platform. For measurements, the three legs are placed on fixed benchmarks that need to be installed at the site of interest. Exact relocation is insured by Kelvin's clamp arrangement – the three feet are wedge-shaped, cone-shaped and flat, and thus there is only one possible way of placing them on the benchmarks (High and Hanna, 1970). The MEM has been adapted for use in coastal environments (Robinson, 1976) and underwater (Askin and Davidson-Arnott, 1981). With the original design, measurements of only three surface

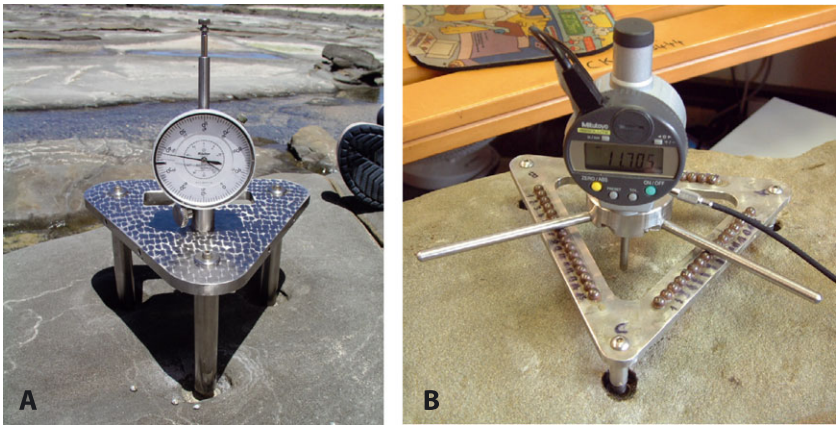

Figure 5. The micro-erosion meter (MEM) (A) and its successor, the traversing micro-erosion meter (T-MEM), a precision point gauging instrument (B). Pictures courtesy of W. Stephenson, who thanks E. Gill for passing on the original MEM instrument.

points could be taken for a given set of benchmarks. Trudgill *et al.* (1981) modified the instrument for a larger number of individual point measurements over an area of up to 200 cm^2. This version of the MEM is known as traversing MEM (T-MEM), which was further improved by Stephenson (1997) by replacing the analog gauge with a digital device with a direct interface to a personal computer for semi-automatic data acquisition. Robinson (1976) and Spate *et al.* (1985) studied errors associated with MEM measurements. Spate *et al.* (1985) identified five possible sources of errors – temperature effects on the instrument, temperature effects on the rock and benchmarks, erosion of the rock by the survey tip (probe erosion), operational irregularity and misuse, and wear of the instrument. They provided a detailed discussion as to how to minimize these errors and published correction equations for the effects of temperature. Since its conception, the MEM has been used in a multitude of scientific studies, focusing on the erosion of shore platforms and of limestone formations (e.g. Trudgill, 1977; Spencer, 1981; Gill and Lang, 1983; Stephenson and Kirk, 1998; Stephenson *et al.*, 2012). An overview of scientific results achieved with the MEM has been given by Stephenson and Finlayson (2009). A version of the T-MEM is commercially available (Albatros Marine Technologies, 2015). The advantage of the MEM is its high precision, which can be in the micrometer range (Spate *et al.*, 1985), the wealth of literature that is available on its use, and the good understanding of the errors associated with the technique. The disadvantages of the MEM are the need for fixed benchmarks installed in the rock, the small area that can be studied with a single benchmark set, and the need for operators to be present to make measurements. The last point means that erosion cannot be observed while it is happening.

Topographic surface measurements

Several technologies have emerged over the last two decades that allow quick high-resolution topographic measurements in the field. Modern laser scanners can obtain hundreds of thousands of data points per second, and photogrammetry techniques have evolved such that good quality topographic data can be generated from pictures taken with hand-held pocket cameras and freely available software (e.g. Fonstad *et al.*, 2013). In addition, remote-controlled drones are now available as platforms for cameras (e.g. Brauchle *et al.*, 2014; Nex *et al.*, 2015), and new concepts, such as range imaging (RIM) (e.g. Nitsche *et al.*, 2013), are emerging. There are a number of techniques available, which can be broadly classified as passive technologies that rely on ambient lighting, or active technologies that rely on the analysis of the reflected return of a signal send by the device. Passive technologies include photogrammetry, while active technologies include lidar, structured light scanning, and RIM. Incidentally, the word lidar is often interpreted as an acronym for 'light detection and ranging' (as already used by Northend, 1967) or 'laser imaging, detection, and ranging', but actually was created by amalgamating the terms light and radar (Ring, 1963).

Photogrammetry has long been used to generate digital elevation models (DEMs) from aerial and satellite images. However, this far-range photogrammetry was of limited use for measuring bedrock erosion – the relatively low resolution and accuracy of the DEMs meant that only large amounts of erosion, such as mass wasting, could be constrained, and good quality cloud-free images covering the right areas at the right times could be difficult and/or expensive to obtain. Nevertheless, the comparison of DEMs calculated from traditional aerial photographs acquired before and after erosion occurred has been used to measure shoreline platform erosion and cliff retreat (Dornbusch *et al.*, 2008), landslides and rockfalls (Bennett *et al.*, 2012), and rapid fluvial incision (Cook *et al.*, 2013).

With the advent of low-cost *unmanned aerial vehicles* (UAVs) and the development of the *structure-from-motion* (SfM) technique and software, photogrammetry has seen a surge in recent years (Fig. 6). SfM enables the creation of three-dimensional (3D) point clouds from randomly oriented photographs without the need for independent camera calibration. A scene can be photographed with a consumer-grade camera either from a range of positions on the ground or using a UAV or both, and the software calculates the position of each photograph and solves for the camera's calibration parameters (Westoby *et al.*, 2012; Fonstad *et al.*, 2013). With UAVs, custom aerial images can be acquired at relatively low cost and a wide range of resolutions can be achieved since resolution depends on the number of pixels in the photographs and the distance between the camera and the object of interest. This allows for the easy and cheap generation of high resolution point clouds with high accuracy (Fig. 6D). An early application of SfM in geomorphology has been described by Heimsath and Farid (2002).

The accuracy of the point cloud scales with the resolution of the images, but is affected by a number of other factors, including image quality, image distortion, camera calibration, image distribution, relief, vegetation, surface texture, and, critically, the number, distribution, and accuracy of ground control points. Systematic large-scale distortions can occur in the calculated topography, generally due to problems in the calculation of camera lens parameters (James and Robson, 2014). Accurately surveyed ground control points can be used to refine the calculation of lens parameters and reduce this distortion, but may not remove it entirely (James and Robson, 2014; Harwin *et al.*, 2015). Distortion is also affected by the orientation of the photographs; it is maximized when the camera orientations are uniform and the images are parallel to each other, and can be reduced by adding oblique images taken from different angles (James and Robson, 2014; Eltner and Schneider, 2015; Harwin *et al.*, 2015). Independent camera calibration may also reduce this effect; however, care must be taken that the calibration is sufficiently robust, otherwise it may reduce the accuracy of the resulting model rather than improve it (Harwin *et al.*, 2015).

With well-distributed ground control points independently measured by total station or differential GPS (James and Robson, 2012; Fonstad *et al.*, 2013; Gómez-Gutiérrez *et al.*, 2014), using simple SfM workflow without extensive camera calibration, accuracies of 5-30 cm can be achieved over areas of the order of 0.1 to 1 km^2. Photogrammetry can also be used at close range to generate topographic data over small areas (square meters) with precision and accuracy of the order of tens of micrometers (Rieke-Zapp, 2010; Beer *et al.*, 2015).

In the past decade, *terrestrial laser scanning* (TLS), a type of lidar instrument, have become a standard tool in geomorphological research (Fig. 6A; for early applications in geomorphology see, e.g. Williams *et al.*, 2000; Bitelli *et al.*, 2004; Nagihara *et al.*, 2004; Schmid *et al.*, 2004). Lidar is an active technology that uses reflected laser pulses to measure the distance between the scanner and objects that reflect the laser beam. Distances can be calculated in several ways. Time of flight scanners simply measure the time between the laser emittance and the arrival of the reflected pulse. Accuracy and precision are typically reported in the range of 6 to 20 mm, and the maximum range can be up to 6 km. Phase shift scanners emit a periodic signal and measure the difference in phase between the emitted and reflected signal, as well as the time of flight. These scanners have greater accuracy and precision (typically 1–3 mm) than time of flight scanners, but shorter range (less than

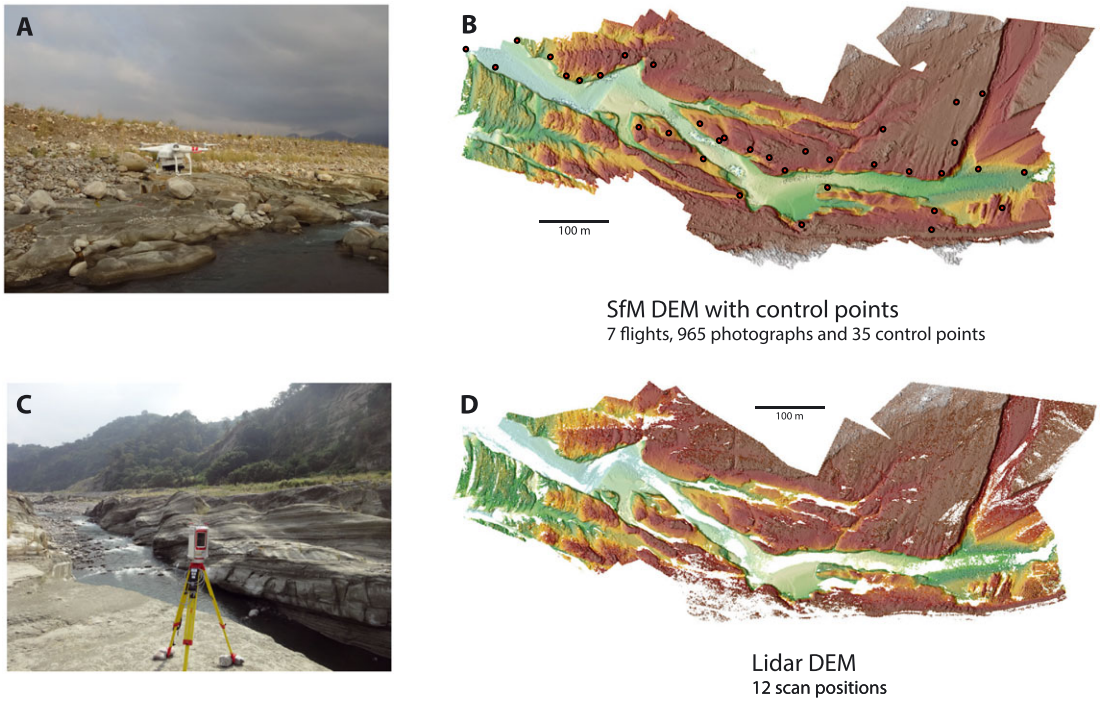

Figure 6. Terrestrial laser scanning (TLS) and unmanned aerial vehicle (UAV)-based structure-from-motion (SfM). (A) A popular UAV for taking areal photographs for SfM and (B) a digital elevation model created using SfM. The coverage is more complete than the lidar data, with a similar degree of surface detail at this resolution. (C) A terrestrial laser scanner and (D) digital elevation model created from TLS data. The surface is represented very accurately, but ground-based measurement in complex terrain often results in areas with no data where the surface was shadowed from view.

300 m). Structured light scanners project a pattern of light on the surface of interest and use the distortion of the pattern to calculate topography. These scanners can have sub-millimeter accuracy and precision, but measure at very short ranges, typically less than 1–2 m (e.g. Wilson *et al.*, 2013).

While individual scans have high accuracy, error can be introduced in the registration process when scans from multiple positions are combined or when scans from different times are compared. Error assessments for laser scanning in fluvial geomorphology have been performed by Heritage and Hetherington (2007) and Hodge *et al.* (2009), while Schaefer and Inkpen (2010) provided error analyses and field protocols specifically for the scanning of rock surfaces. There are a number of examples for the use of terrestrial laser scanning in bedrock erosion studies (e.g. Williams *et al.*, 2000; Wilson *et al.*, 2013; Cook *et al.*, 2014; Beer *et al.*, 2015; Vann Jones, née Norman EC *et al.*, 2015).

RIM is a relatively new active time-of-flight technology for surface-distance measurements. Commercial RIM cameras are available since the mid-1990s (Lange and Seitz, 2001). The instrument is constructed similar to a camera, but in addition to brightness data, distance information is recorded for each individual pixel. The advantages of RIM cameras are the light design, making it highly mobile even in difficult terrain, and the high recording frequency. RIM cameras can be operated in video mode, taking images at rates of 25 to 50 Hz, allowing for quick data acquisition and for the near real-time monitoring of processes. Kolb *et al.* (2010) provided a recent review of the RIM technology, and Nitsche *et al.* (2010, 2013 published a detailed error analysis for outdoor use, and experimental protocols in the context of geomorphology.

In order to use the earlier mentioned techniques to measure erosion, data obtained at different times must be compared in a robust way. This can introduce additional sources of error, particularly for complex topography. For a thorough discussion of these issues, see Lague *et al.* (2013). The most common method of topographic comparison is to create DEMs from point clouds measured at different times, then subtract the DEMs to obtain a DEM of difference (DoD). While this approach is straightforward and well-suited to some questions, it does have some drawbacks. First, creating a DEM takes raw data that is often irregularly distributed and merges and interpolates points as necessary to create a regularly spaced grid. This can introduce errors depending on the roughness of the surface, gaps in the point cloud, and the resolution of the data. Second, because in DEMs, a single height value is associated with each location, differences can only be calculated normal to a single fixed plane. This gives only vertical erosion rates, and creates problems for complex surfaces including for example overhangs or vertical walls.

Another possible method of comparison is to create a triangulated mesh from one or both point clouds and calculate either a mesh-mesh distance or a point cloud-mesh distance in a direction normal to the local reference surface. This has the advantage of capturing surface-normal erosion rates, rather than merely vertical erosion rates. Disadvantages are that meshes can be unwieldy to work with and that creating a mesh of a complicated surface (i.e. with overhangs) is a non-trivial task and can require expensive software. Meshes are also a form of interpolation of the original point cloud, somewhat removed from the raw data.

Cloud-to-cloud comparisons have the advantage of working with the original data, which avoids issues of interpolation. The recent development of freely available software to perform cloud-to-cloud comparisons makes this technique more feasible. The open-source software CloudCompare (CloudCompare 2.5, 2014) allows for the calculation of closest-point differences between two point clouds among many other functions. A more sophisticated technique is implemented in the M3C2 algorithm (Lague *et al.*, 2013), which is now available within CloudCompare. M3C2 first determines optimal normal vectors for a subset of points, then calculates the distance between the two point clouds along a cylinder of a given radius projected in the direction of the normal. In addition to the

distances, uncertainties and confidence levels are calculated, allowing for more robust interpretation of apparent changes (Lague *et al.*, 2013).

Catchment-scale measurements

Measurements of denudation are made on the catchment scale, and typically consist of the quantification of the total volume of material that has been evacuated from the considered area over a given time period. The discharge in a channel integrates all the processes that happen upstream. Thus, by measuring the water chemistry or solid load in a stream one can obtain information on catchment-wide denudation rates. A river can transport the products of erosion in three modes: as dissolved load, as suspended load, and as bedload. The latter two modes of transport together constitute the particulate load. When travelling as suspended load, the sediment particles are kept in suspension by turbulent forces of the water flow, while bedload particles travel along the bed by sliding, rolling or hopping. Whether a particle travels as suspended load or bedload depends on the local hydraulics as well as on the particle size. Depending on the geography and geology of the area and on the characteristics of the transporting flood, each of the three modes of transport can be dominant. For instance, the dissolved load can be substantial in catchments that feature chemically reactive rocks such as evaporites or limestone or where physical erosion rates are small (e.g. Lana-Renault and Regüés, 2007), while bedload can dominate over suspended load in mountain rivers or during large floods (Turowski *et al.*, 2010).

We can identify seven different types of strategies that have been used to obtain denudation rates, namely *surveying the deposition in natural or man-made reservoirs, rating curve construction and temporal upscaling, landslide mapping, chemical fingerprinting, cosmogenic nuclide dating* of sand samples, *thermochronology,* and the analysis of sedimentary records in deposition areas. These strategies are outlined.

Surveying the deposition in reservoirs

If a reservoir, be it natural or man-made, is a complete sink for all the sediment that leaves a catchment, deposition rates can be estimated from geometric changes of the deposited material. This is typically done from repeated bathymetric surveys using either a meter stick from a boat in small reservoirs (e.g. Lauffer and Sommer, 1982; Nitsche *et al.*, 2011), sonar or acoustic profiling (e.g. Lenzi *et al.*, 1990; Poppe *et al.*, 2006) or aquatic-terrestrial lidar (e.g. Hilldale and Raff, 2007; McKean *et al.*, 2009). Continuous measurements of changes in deposited sediment masses have been made by equipping sediment retention basins with what are essentially big weighing scales (e.g. Lauffer and Sommer, 1982; Rickenmann and McArdell, 2008). Siltation rates for European reservoirs have been compiled by Vanmaercke *et al.* (2011).

Rating curve construction and temporal upscaling

For the rating curve construction method, concurrent measurements of channel discharge and of the flux of the erosion products need to be made at a site. A relationship is fitted to the data, which is then extrapolated to unmeasured discharges, and used as a predictive model. By integrating data series of discharge spanning a longer interval than was measured with the fitted relationship, the sediment outflux from the area is calculated. In this way yearly to centennial denudation rates can be obtained, depending on the length of the available discharge time series. A full review of sampling techniques and strategies for the sediment load of rivers is beyond the scope of the present article and we only give a brief overview here. The reader is directed to more specialized reviews for further details (e.g. Reid *et al.*, 1997; see also the reviews pointed out in the specific subsections later).

The suspended load of a river is thought to be determined by supply conditions (e.g. Vanoni, 1975). Concentrations are commonly modeled as a power function of discharge, the parameters of which are site specific. Currently, no generally accepted methods exist for predicting these parameters for ungauged sites (Asselman, 2000). The situation is similar for dissolved load measurements. Both dissolved and suspended load concentrations can be measured directly by filtering water samples, and by chemically analyzing the filtered water and drying and weighing the remaining solids. In many streams, concentrations vary with depth and across the channel, and integrated sampling strategies and interpolation techniques have been developed to account for this (e.g. Eads and Thomas, 1983; Bouchez *et al.*, 2011). For higher temporal resolution of suspended solids, turbidity probes calibrated to the material in the stream of interest can be used (e.g. Fleming, 1969). There are standard protocols available for stream water sampling, and the errors involved are fairly well understood (e.g. Walling and Webb, 1981, 1987; Holtschlag, 2001; Schleppi *et al.*, 2006; Chan *et al.*, 2008; Rasmussen *et al.*, 2009).

It is generally thought that, in contrast to dissolved and suspended load transport, bedload transport is predictable by semi-empirical equations (e.g. Vanoni, 1975). However, the predictive quality of such equations for mountain rivers especially is poor, and field data are scarce (e.g. Reid *et al.*, 1997; Nitsche *et al.*, 2011; Yager *et al.*, 2012; Schneider *et al.*, 2015). In general, there are five different strategies for measuring bedload transport. First, moving bedload material can be caught in traps placed in or on the stream bed. The popular Helley–Smith sampler (Helley and Smith, 1971), the Bunte-type bedload traps (Bunte *et al.*, 2004), and the Birkbeck-type samplers (Reid *et al.*, 1980) fall into this category. Second, the regular survey of natural or man-made reservoirs can yield information on the long-term export of bedload material from a catchment (e.g. Rickenmann *et al.*, 2012). Third, the use of tracer particles can yield detailed information on the transport process (e.g. Hassan, 1990; Schneider *et al.*, 2014), but needs to be complemented by measurements of the active layer thickness to calculate solid fluxes (Haschenburger and Church, 1998). Fourth, differences in topographic measurements from before and after an event can help to constrain the total out- or through-flux of material (e.g. Lane *et al.*, 1995; Heimann *et al.*, 2014). And fifth, indirect or surrogate measurements, for instance of the acoustic or seismic noise generated by bedload motion, can be used to obtain information on relative transport rates (e.g. Burtin *et al.*, 2011; Rickenmann *et al.*, 2014). General reviews of methods to measure bedload transport have been given by Reid *et al.* (1997), and Ergenzinger and de Jong (2003). Bunte *et al.* (2004) reviewed portable traps, while Gray *et al.* (2010), Rickenmann (2015) and Burtin *et al.* (2016) focused on surrogate methods.

Finally, the relation between the three components of the transported load, i.e. the dissolved load, the suspended load and the bedload, is highly variable and incompletely understood (e.g. Meunier *et al.*, 2006). The often applied focus on suspended sediment is not warranted for many types of rivers. Currently, no generally valid methods exist that allow the prediction of an unmeasured component from a measured one. For a review of the partitioning between suspended load and bedload see Turowski *et al.* (2010).

The method of rating curve construction is associated with some common pitfalls, some of which are related to the fitting of regression equations, which is less straight forward than often thought, especially if the model of choice is non-linear

(e.g. Mark and Church, 1977; Clauset *et al.*, 2009; Domeneghetti *et al.*, 2012). Non-linear fitting procedures based on the method of least squares usually operate under the assumption that errors are normally distributed, which is not generally true for environmental data. When log-transforming the data and fitting a linear model, the assumption of normally distributed errors becomes one of log-normally distributed errors, which is often a better description for non-negative quantities such as stream discharge or sediment concentration. However, this method leads to log-transform bias (Miller, 1984), which arises because fitting procedures typically work with the median of the data, but in prediction the mean is of interest. Because the error distribution is skewed after log-transforming the data, mean and median are not the same anymore, and using the regression model for prediction results in an underestimation of the load (Ferguson, 1986). However, the log-transform bias can be corrected for when the original data are available (Miller, 1984; Ferguson, 1986). An alternative to least-squares regression is maximum likelihood estimation, which can be advantageous in some circumstances (e.g. Clauset *et al.*, 2009; Gaeuman *et al.*, 2015).

Another group of problems is related to the extrapolation of the derived rating curves. High discharges often contribute disproportionally to total sediment export (e.g. Kirchner *et al.*, 2001), while data are commonly only available for small and intermediate discharges. Similarly, sediment export can change over time, for example seasonally (e.g. Mao *et al.*, 2014), after extreme floods (e.g. Turowski *et al.*, 2009), or in response to external events such as a volcanic eruption (e.g. Lehre *et al.*, 1983) or an earthquake (e.g. Hovius *et al.*, 2011). Thus, the behavior of the catchment needs to be well understood to ensure that representative samples for the timescale of interest are taken.

Landslide mapping

The *landslide mapping* method for denudation measurement works in regions where landsliding is the dominant mass wasting process, and where hillslope erosion by other processes is negligible in comparison. These conditions generally apply in steep mountain terrain in tectonically active regions with a humid climate (Hovius *et al.*, 1997), but may also be true for other regions. Landslide scars can be mapped from satellite pictures or air photographs, and they are particularly easy to recognize in regions with dense vegetation. Automatic mapping algorithms are available (e.g. Behling *et al.*, 2014), but their quality varies (e.g. Marc and Hovius, 2015). Two elements are necessary in converting mapped scar areas into a landscape-wide denudation rate. The first of these is a relationship between scar area and landslide volume (Stark and Hovius, 2001; Malamud *et al.*, 2004; Larsen *et al.*, 2010), which is highly dependent on the properties of the soil and the bedrock in the region of interest, and is thus site-specific and difficult to generalize. The ability to distinguish between the erosional and depositional parts of the scar may also affect the accuracy of this conversion (e.g. Larsen *et al.*, 2010). For the estimation of long-term denudation rates, the second necessary element is the frequency–magnitude relation of the landslides. Typically, mapping only covers a short span of time, and both the largest and rarest landslides and the smallest ones that are most difficult to map may be of equal importance in setting total eroded volumes (Stark and Hovius, 2001). When considering erosion due to a single event, e.g. an earthquake (e.g. Hovius *et al.*, 2011; Li *et al.*, 2014), the completeness and accuracy of the mapping is important (Malamud *et al.*, 2004; Marc and Hovius, 2015; Marc *et al.*, 2016).

Chemical fingerprinting

Chemical fingerprinting provides a method to complement existing measurements on parts of the erosive export, for instance suspended load and dissolved load, by an estimation of the unmeasured parts. It relies on the notion that the average chemical composition of the exported material should correspond to the known composition of the source materials. Thus, the ratios of the abundance of certain elements can be used to back-calculate the sum of material lost in transport (by deposition or chemical reactions) and unmeasured parts. The method has been applied to complement the erosional budget of the Himalayas (Galy and France-Lanord, 2001; Lupker *et al.*, 2012).

Cosmogenic nuclide basin-wide denudation rates

As discussed earlier, *in situ cosmogenic nuclides* are produced in certain materials at or near the surface at predictable rates. The production of cosmogenic isotopes decays exponentially with depth, with the quickness of decay dependent on the density of the overlying material. As material approaches the surface, it accumulates cosmogenic isotopes; if the material has been moving towards the surface at a constant rate during its residence time in the near-surface, then the rate of denudation can be obtained by measuring the concentration of these isotopes. Because the isotopes accumulate during the sample's trip to the surface, the integration time of the measured concentrations is inversely dependent on the denudation rate - faster denudation is measured over shorter timescales. Thus, care must be taken when interpreting variations in cosmogenic denudation rates, as they are, by definition, sampling different lengths of time (Bierman and Steig, 1996).

This technique can be used to measure denudation rates at point locations, allowing for the exploration of spatial variability in denudation rates (Bierman and Nichols, 2004; Heimsath 2006). One can also take advantage of the hydrologic system and the natural mixing that occurs during the transport of sediment in fluvial systems by sampling river sand (Granger *et al.*, 1996; Lupker *et al.*, 2012; Granger and Riebe, 2014). The concentration of cosmogenic isotopes in such a sand sample provides an average denudation rate for the drainage area upstream of the sampling location, provided that a number of assumptions are met, including steady denudation rates over the integration time period, representative and well-mixed sediment at the sampling point, and negligible post-erosion accumulation of isotopes (during transport or temporary storage), and an even (or known) distribution of the relevant mineral throughout the catchment (Granger and Riebe, 2014). Caution must be taken to assess whether the above assumptions are valid for the catchment of interest; otherwise the isotope concentration will not yield a meaningful rate. Violations of the assumptions commonly arise from the presence of landsliding in the catchment (Niemi *et al.*, 2005).

Thermochronology

Denudation on longer timescales can be constrained using low-temperature thermochronometers such as fission tracks, (U-Th)/He, $^{40}Ar/^{39}Ar$, and, in a recent development, optically stimulated luminescence (Reiners and Brandon, 2006; Herman *et al.*, 2010). These systems rely on the temperature-dependent diffusion of radioactive decay products or annealing of damage resulting from decay (fission tracks). At high temperatures, daughter products diffuse and fission tracks anneal quickly and do not accumulate, while at low temperatures diffusion and annealing are negligible and daughter products and fission tracks accumulate. The temperature that separates these two regimes is known as the closure temperature of the system, and depends on the diffusion kinetics of the system, as well as on the cooling rate of each sample. Thus, the concentration of

daughter products or fission tracks in a sample depends on the amount of time that the sample has spent below the closure temperature, and can therefore be used to calculate a cooling rate for the sample. In a region experiencing exhumation in the absence of thermal perturbations, cooling is the result of the movement of material towards the surface and cooling ages can provide information about exhumation rates. The closure temperatures of commonly used systems range from 60 °C (apatite (U-Th)/He) to 350 °C (muscovite $^{40}Ar/^{39}Ar$) (Reiners and Brandon, 2006), providing information on exhumation from depths of ~2 to ~12 km for a geothermal gradient of 30 °C/km. Of particular interest for studies of erosion is the recent development of OSL in quartz as a thermochronometer with closure temperature of 30 to 35 °C (Herman *et al.*, 2010). As with cosmogenic erosion rates, the timescale of thermochronology-based exhumation rates depends on the rate, with faster exhumation measured over shorter timescales. However, the availability of multiple thermochronometric systems with a range of closure temperatures means that cooling and exhumation can be constrained over multiple timescales in a single sample (eg. Avdeev and Niemi, 2011; Herman *et al.*, 2013).

Thermochronology can be used on single samples to estimate exhumation rate if the geothermal gradient is known or assumed. Age-elevation transects, multiple samples collected over a range of elevations, do not require knowledge of the geothermal gradient, but require assumptions about the geometry of the isotherms and the path of the samples through them. Detrital thermochronology in a sedimentary sequence can also be used to constrain the exhumation of the sediment source through time (Reiners and Brandon, 2006; Rahl *et al.*, 2007). Low temperature systems such as apatite (U-Th)/He can be perturbed by the development of relief and have been used to constrain canyon incision in a range of settings (House *et al.*, 1998; Schildgen *et al.*, 2007, Flowers and Farley, 2012). Apatite $^{4}He/^{3}He$ analysis, a more sophisticated method using the distribution of both radiogenic and stable Helium in single crystals, has also been used to constrain glacial erosion (Shuster *et al.*, 2005), canyon incision (Flowers and Farley, 2012), and relief development (Valla *et al.*, 2012).

Sedimentary records

Sedimentary records present an extension of the measurement of denudation by constraining the sediment volumes delivered to a depositional area. In essence, the volume deposited in the stratigraphic unit above a datable layer has to be estimated and the deposition rate can be calculated by dividing by its age. The erosion rate in the catchment supplying the material can be obtained by assuming it is equal to the deposition rate, thus neglecting transfer times and catchment-internal storage of sediment. Sometimes, there is a stratigraphic layer containing a marker deposit such as volcanic ash from a known eruption, providing a reliable date (Lowe, 2011). Some deposits have a yearly lamination, known as varves, and by counting these layers, precise dates can be obtained (e.g. Zolitschka, 2003; Ojala *et al.*, 2012). Otherwise, one can use ^{14}C, magnetostratigraphic or fossil dating, or, in suitable circumstances, other dating techniques described earlier.

Some General Tips and Pitfalls to be avoided

Environmental conditions and their effect on measurements

Many measurements are affected by the ambient environmental conditions. For instance, the speed of light is dependent on air temperature and pressure, and on relative humidity, and thus also on height above sea level. This affects the accuracy and precision of all survey instruments that work with the time-of-flight principle, such as terrestrial laser scanners. Modern instruments either directly measure the relevant parameters, or provide an interface for the user to enter them. All materials, particularly metals, but also the rock itself, expand and contract in response to temperature changes. Similarly, electronic sensors often deliver a temperature-sensitive output. Depending on the specific aim of the campaign and the desired precision, these effects may be negligible. If not, often, such changes can be corrected for, if the relevant relations and the local temperatures are known. In any case, we recommend to record at least three temperatures routinely in any measurement campaign concerned with erosion. First, the air temperature, second, the ground temperature, be it of bedrock or of soil, and third an instrument-specific temperature. This could be the surface temperature of the metal parts for example of point gauging instruments, or the temperature of the sensors and electronic boards. A further point worth considering are ambient lighting conditions that can affect the precision of active instruments specifically (e.g. RIM; see Nitsche *et al.*, 2013), but can also be important for instance in photogrammetric measurements (Trinder *et al.*, 1995). Laboratory experiments under controlled conditions help to understand instrument behavior, and can be used to constrain corrective functions. A number of other environmental parameters, e.g. wind, moisture content and surface wetness, might affect accuracy or precision of specific methods.

Clock synchronization

In campaigns where several instruments operate side by side and record at high temporal resolution, for example to constrain both erosion rates and driving conditions, it is crucial to regularly synchronize the clocks of the loggers (e.g. Beer *et al.*, 2015). In general, it is preferable to store all data within the same logger system, such that synchronization problems do not arise in the first place. However, this may not be possible, e.g. due to physical separation of various sensors. For systems that operate independently for long time periods, where manual synchronization is not possible on a regular basis, GPS may be a convenient means to obtain a global time. This method is routinely used in seismic campaigns, and ready solutions are available.

Instrument drift

Instrument drift, i.e. a systematic trend in the measurement over time that is unrelated to the properties that are measured, can arise for wide variety of reasons. Examples are gradual wear of springs in force balances, temperature-dependent shifts over a survey day or season, tip wear of point gauges, and aging of electronics. Instrument drift can be detected by comparing measurements to a stable benchmark. The measurement strategy can also help to detect drift and minimize its effect. For example, if measuring along a linear transect, drift will be impossible to spot when all measurements are made in order along the line, but by switching to and fro the different ends, drift may be detected (see Squires, 1998).

The value of experience: understanding the method

Before going into the field to obtain high precision data, it is necessary to get to know the instrument and the measurement

condition. In the best case, a researcher new to a technique should work together with someone with experience. Of course, this is not always possible, especially for purpose-designed instruments. A series of experiments under controlled conditions for studying the instrument's behavior and its response to temperature, ambient light, wetness, or other environmental situations, and to constrain errors, should be mandatory before using any instrument in the field, whether it is purchased or purpose-built. Technical specifications given in manuals do not necessarily match the parameters of the instrument and the specific purpose it is applied for, and it should be checked that the desired criteria are met. We also recommend obtaining a basic knowledge of the technical and physical principles behind the measurement to be made. Such knowledge can help to judge the range of operational conditions, to protect from making simple operational mistakes and from misinterpreting the data.

Selection bias and effects of the measurement procedure on what is to be measured

Selection bias arises when the measurement returns biased results due to decisions made for the measurement strategy. Most often, this results either from the design of the instrument, or from the decision of where to make a measurement. For instance, when erosion rates are consistently and only measured in areas where fast erosion occurs, the measured mean overestimates the true mean for the entire landscape. Further examples for the effects of the measurement on what is to be measured are instruments that protrude into the flow driving the erosion and therefore alter the local flow field, or the introduction of micro-cracks into the bedrock by drilling during the installation of benchmarks or instruments. Both selection bias and measurement effects can be subtle. The best protection from these effects is a clear theoretical picture of the process to be studied, a good knowledge of the measurement method and instrumentation, an established hypothesis that is to be tested, and general care in designing and executing the measurements.

The Sadler effect

A specific statistical effect has been identified by Sadler (1981, 1999) that arises when data of deposition or erosion relating to different timescales are compared. When sedimentation rates are plotted against the time span over which they are measured, a clear trend becomes visible: low sedimentation rates correspond to long timescales and vice versa. The effect arises because deposition is not a continuous process, but episodes of activity alternate with episodes of hiatus. As the measurement timescale increases, longer hiatuses are incorporated, and the observed scaling between deposition rates and timescale can be obtained when the periods of hiatus is described by a heavy-tailed distribution (Schumer and Jerolmack, 2009). The Sadler effect has been shown to be present also in erosional environments, where the longest timescales correspond to the highest erosion rates (Gardner *et al.*, 1987; Finnegan *et al.*, 2014). Some methods, for instance catchment-wide denudation measurements based on cosmogenic nuclides, are not susceptible to the Sadler effect (Willenbring and von Blanckenburg, 2010a). The Sadler effect needs to be considered especially when comparing erosion rates measured with different techniques or over different timescales, or when measured rates are interpreted in a wider context.

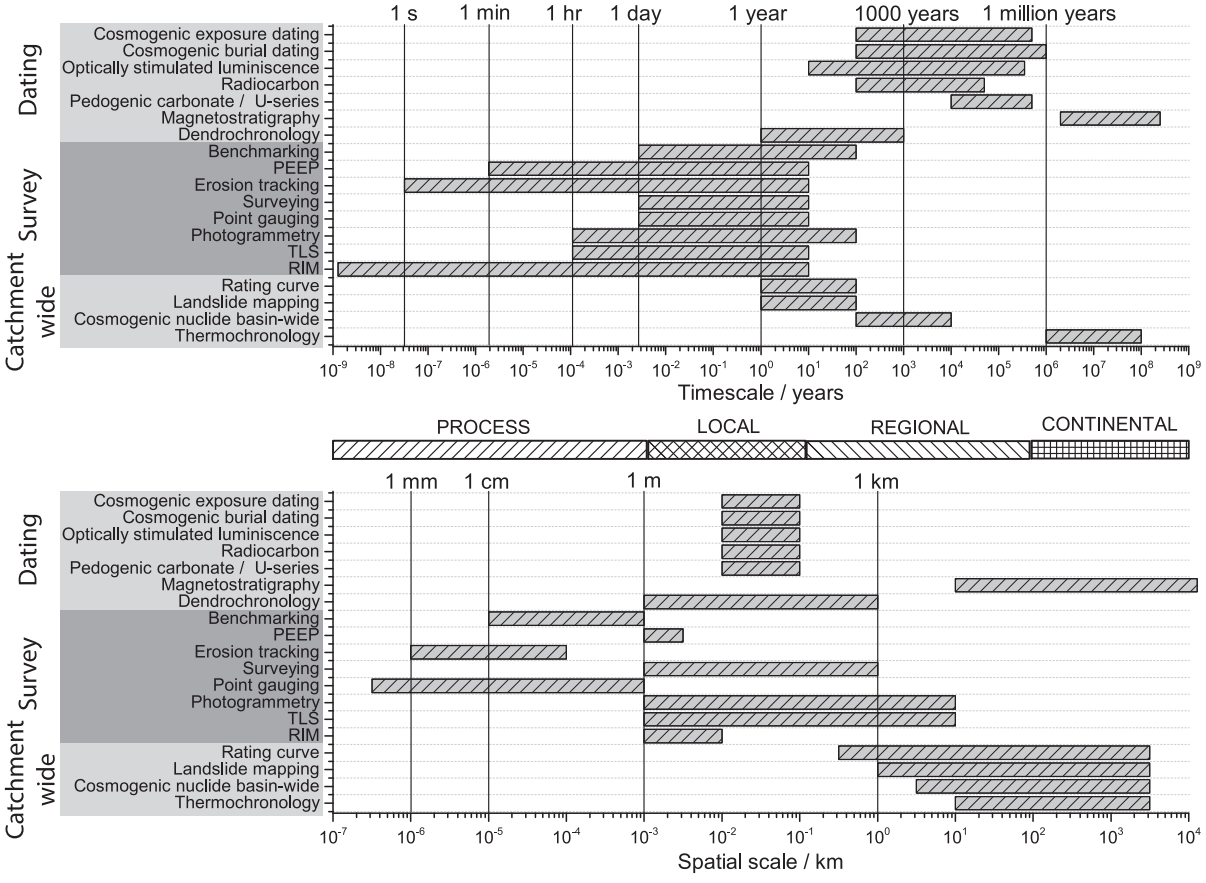

Figure 7. Temporal and spatial scales the various methods can be applied for.

Concluding Remarks

We live in an exciting time. Cosmogenic nuclide dating has been established as a standard tool in the study of erosion, lidar instruments and structure from motion allow easy measurements of topography in unprecedented detail, and new methods, such as resistance tracking, allow high resolution measurement that have not been possible just a decade ago. Here, we have assembled many methods that have been developed to measure bedrock erosion and denudation in the field and highlighted their relative merits and their range of applicability. To choose a method suitable for her or his research, the scientist should consider both the scientific aim of the study and the location where it is to be conducted. The different methods apply to different temporal and spatial scales (Fig. 7). Temporal scales can range from less than a second to millions of years (Fig. 7A). Spatial scale can vary from the process scale (micrometers to meters) to the local (meters to hundreds of meters), regional (hundreds of meters to hundreds of kilometers) to the continental and global scale (thousands of kilometers) (Fig. 7B). Some methods can be applied only at regional to continental spatial scales and need data series that range back thousands or millions of years, such as magnetostratigraphy. The choice of method is also determined by the necessary precision. For example, the erosion rate at a given location may be lower than what can be measured by any of the survey methods within the duration of the project. Likewise, if erosion happens during rare extreme events, one may not be lucky enough to observe one. In these cases one needs to resort to methods that work on longer timescales, which has the advantage of averaging over the full magnitude frequency distribution of erosion events. However, to unravel the details of the erosion processes, high temporal and spatial resolution is usually necessary. In the end, studies on different spatial and temporal scales complement each other and are necessary for a full comprehension of bedrock erosion in nature.

Acknowledgements—The authors thank A. Beer, N. Hovius and W. Stephenson for providing pictures illustrating some techniques they have developed and used. S. Lane encouraged the authors to write this review and was patient enough not to change his mind over the lengthy writing process. A. Beer, R. Emberson and J. Scheingross provided helpful comments on an earlier version of this manuscript, and two anonymous reviewers gave detailed criticisms that greatly improved the paper.

References

Albatros Marine Technologies. 2015. Traverse micro erosion meter (TMEM). http://albatrosmt.com/products/ [July 2016]

Anderson RS, Anderson SP. 2010. Geomorphology – The Mechanics and Chemistry of Landscapes, first edition. Cambridge University Press: Cambridge.

Anderson JM, Mikhail EM. 1998. Surveying, Theory and Practice, seventh edition. WCB/McGraw-Hill: Columbus, OH.

Askin RW, Davidson-Arnott RGD. 1981. Micro-erosion meter modified for use under water. *Marine Geology* **40**: M45–M48.

Asselman NEM. 2000. Fitting and interpretation of sediment rating curves. *Journal of Hydrology* **234**: 228–248.

Avdeev B, Niemi NA. 2011. Rapid Pliocene exhumation of the central Greater Caucasus constrained by low-temperature thermochronometry. *Tectonics* **30**: TC2009. DOI:10.1029/2010TC002808.

Barke R, Lamb S. 2006. Late Cenozoic uplift of the Eastern Cordillera, Bolivian Andes. *Earth and Planetary Science Letters* **249**: 350–367.

Beer AR, Turowski JM. 2015. Bedload transport controls bedrock erosion under sediment-starved conditions. *Earth Surface Dynamics* **3**: 291–309. DOI:10.5194/esurf-3-291-2015.

Beer AR, Turowski JM, Fritschi B, Rieke-Zapp D. 2015. Field instrumentation for high-resolution parallel monitoring of bedrock erosion and bedload transport. *Earth Surface Processes and Landforms* **40**: 530–541. DOI:10.1002/esp.3652.

Beer AR, Turowski JM, Kirchner JW. 2016. Graffiti for science – erosion painting reveals spatially variable erosivity of sediment-laden flows. *Earth Surface Dynamics Discussions.* DOI:10.5194/esurf-2016-27.

Behling R, Roessner S, Kaufmann H, Kleinschmit B. 2014. Automated spatiotemporal landslide mapping over large areas using RapidEye time series data. *Remote Sensing* **6**: 8026–8055. DOI:10.3390/rs6098026.

Bennett G, Molnar P, Eisenbeiss H, McArdell B. 2012. Erosional power in the Swiss Alps: characterization of slope failure in the Illgraben. *Earth Surface Processes and Landforms* **37**: 1627–1640. DOI:10.1002/esp.3263.

Berg RR, Gangi AF. 1971. Bubnoff unit: An objection. *Geological Society of America Bulletin* **82**: 3475–3476.

Berger C, McArdell BW, Fritschi B, Schlunegger F. 2010. A novel method for measuring the timing of bed erosion during debris flows and floods. *Water Resources Research* **46**: W02502. DOI:10.1029/2009WR007993.

Berger C, McArdell BW, Schlunegger F. 2011. Direct measurement of channel erosion by debris flows, Illgraben, Switzerland. *Journal of Geophysical Research* **116** . DOI:10.1029/2010JF001722.F01002

Bierman PR, Nichols KK. 2004. Rock to sediment – slope to sea with ^{10}Be- rates of landscape change. *Annual Review of Earth and Planetary Sciences* **32**: 215–255. DOI:10.1146/annurev.earth.32.101802.120539.

Bierman P, Steig EJ. 1996. Estimating rates of denudation using cosmogenic isotope abundances in sediment. *Earth Surface Processes and Landforms* **21**: 125–139.

Bierman PR, Marsella KA, Patterson C, Davis PT, Caffee M. 1999. Mid-Pleistocene cosmogenic minimum-age limits for pre-Wisconsinan glacial surfaces in southwestern Minnesota and southern Baffin Island: a multiple nuclide approach. *Geomorphology* **27**: 25–39. DOI:10.1016/S0169-555X(98)00088-9.

Bitelli G, Dubbini M, Zanutta A. 2004. Terrestrial laser scanning and digital photogrammetry techniques to monitor landslide bodies. In *Proceedings of the XXth ISPRS Congress*, Istanbul; 6.

Bouchez J, Métivier F, Lupker M, Maurice L, Perez M, Gaillardet J, France-Lanord C. 2011. Prediction of depth-integrated fluxes of suspended sediment in the Amazon River: particle aggregation as a complicating factor. *Hydrological Processes* **25**: 778–794. DOI:10.1002/hyp.7868.

Brauchle J, Rüther-Kindel W, Berger R. 2014. MACS-TumbleCam – a novel approach for aerial oblique imaging. *Photogrammetrie, Fernerkundung, Geoinformation* **4**: 253–263. DOI:10.1127/1432-8364/2014/0241.

Bunte K, Abt SR, Potyondy JP, Ryan SE. 2004. Measurement of coarse gravel and cobble transport using portable bedload traps. *Journal of Hydraulic Engineering* **130**(9): 879–893. DOI:10.1061/(asce)0733-9429(2004)130:9(879.

Burbank DW, Leland J, Fielding E, Anderson RS, Brozovic N, Reid MR, Duncan C. 1996. Bedrock incision, rock uplift and threshold hillslopes in the northwestern Himalayas. *Nature* **379**: 505–510.

Burtin A, Cattin R, Bollinger L, Vergne J, Steer P, Robert A, Findling N, Tiberi C. 2011. Towards the hydrologic and bed load monitoring from high-frequency seismic noise in a braided river: The "torrent de St Pierre", French Alps. *Journal of Hydrology* **408**: 43–53. DOI:10.1016/j.jhydrol.2011.07.014.

Burtin A, Hovius N, Turowski JM. 2016. Seismic monitoring of geomorphic processes. *Earth Surface Dynamics* **4**: 285–307. DOI:10.5194/esurf-4-285-2016.

Candy I, Black S, Sellwood BW. 2004. Quantifying time series of pedogenic calcrete formation using U-series disequilibria. *Sedimentary Geology* **170**: 177–187.

Carrara PE, Carroll TR. 1979. The determination of erosion rates from exposed tree roots in the Piceance Basin, Colorado. *Earth Surface Processes* **4**: 307–317.

Chan L, Li Y, Stenstrom MK. 2008. Protocol evaluation of the total suspended solids and suspended sediment concentration methods: solid recovery efficiency and application for stormwater analysis. *Water Environment Research* **80**: 796–805. DOI:10.2175/106143008X296497.

Chatanantavet P, Parker G. 2011. Quantitative testing of model of bedrock channel incision by plucking and macroabrasion. *Journal of Hydraulic Engineering* **137**: 1311–1317. DOI:10.1061/(ASCE)HY.1943-7900.0000421.

Clarke ML, Rendell HM. 2006. Process–form relationships in Southern Italian badlands: erosion rates and implications for landform evolution. *Earth Surface Processes and Landforms* **31**: 15–29. DOI:10.1002/esp.1226.

Clauset A, Shalizi CR, Newman MEJ. 2009. Power-law distributions in empirical data. *SIAM Rev.* **51**(4): 661–703. DOI:10.1137/070710111.

CloudCompare 2.5. 2014. CloudCompare (version 2.5) [GPL software]. EDF R&D, Telecom ParisTech. http://www.cloudcompare.org/ [July 2016].

Colbert EH. 1956. Rates of erosion in the Chinle Formation. *Plateau* **28**(4): 73–76.

Colby BR. 1964. Scour and Fill in Sand-bed Streams. In United States Geological Survey Professional Paper 462-D. US Geological Survey: Reston, VA; 32.

Cook KL, Turowski JM, Hovius N. 2013. A demonstration of the importance of bedload transport for fluvial bedrock erosion and knickpoint propagation. *Earth Surface Processes and Landforms* **38**: 683–695. DOI:10.1002/esp.3313.

Cook KL, Turowski JM, Hovius N. 2014. River gorge eradication by downstream sweep erosion. *Nature Geoscience* **7**: 682–686. DOI:10.1038/NGEO2224.

Craddock WH, Kirby E, Harkins NW, Zhang H, Shi X, Lui J. 2010. Rapid fluvial incision along the Yellow River during headward basin integration. *Nature Geoscience* **3**: 209–213. DOI:10.1038/NGEO777.

Craddock WH, Kirby E, Zheng D. 2012. Tectonic setting of Cretaceous basins in NE Tibet: Insights from Jungong basin. *Basin Research* **24**(1): 51–69. DOI:10.1111/j.1365-2117.2011.00515.x.

De Jong C. 1992. Measuring changes in micro and macro roughness on mobile gravel beds. In *Erosion and Sediment Transport Monitoring Programmes in River Basins* (Proceedings of the Oslo Symposium, August 1992), IAHS Publication 210. IAHS Press: Wallingford; 31–40.

Della Seta M, Del Monte M, Fredi P, Lupia PE. 2007. Direct and indirect evaluation of denudation rates in Central Italy. *Catena* **71**: 21–30. DOI:10.1016/j.catena.2006.06.008.

Dethier DP. 2001. Pleistocene incision rates in the western United States calibrated using Lava Creek B tephra. *Geology* **29**: 783–786. DOI:10.1130/0091-7613(2001)029<0783:PIRITW>2.0.CO;2.

DeVries P, Burges SJ, Daigneau J, Stearns D. 2001. Measurement of the temporal progression of scour in a pool-riffle sequence in a gravel bed stream using an electronic scour monitor. *Water Resources Research* **37**(11): 2805–2816. DOI:10.1029/2001WR000357.

Dietrich WE, Nelson PA, Yager E, Venditti JG, Lamb MP. 2005. Sediment patches, sediment supply, and channel morphology. In In *4th Conference on River, Estuarine, and Coastal Morphodynamics*. A.A. Balkema Publishers: Rotterdam.

Domeneghetti A, Castellarin A, Brath A. 2012. Assessing rating-curve uncertainty and its effects on hydraulic model calibration. *Hydrology and Earth System Science* **16**: 1191–1202. DOI:10.5194/hess-16-1191-2012.

Dornbusch U, Robinson DA, Moses CA, Williams RBG. 2008. Soft copy photogrammetry to measure shore platform erosion on decadal time scales. *Journal of Coastal Conservation* **11**: 193–200.

Dubille, M. 2009. *Sediment Transport and Abrasion in Bedrock Rivers – From Measurements to Models on an Himalayan Example*, PhD Thesis. Joseph Fourier University, Grenoble (in French).

Duncan SH, Ward JW. 1985. A technique for measuring scour and fill of salmon spawning riffles in headwater streams. *Water Resources Bulletin* **21**(3): 507–511.

Dunne T, Dietrich WE, Brunengo MJ. 1978. Recent and past erosion rates in semi-arid Kenya. *Zeitschrift für Geomorphologie, Neue Folge, Supplement Band* **29**: 130–140.

Eads RE, Thomas RB. 1983. Evaluation of a depth proportional intake device for automatic pumping samplers. *Water Resources Bulletin* **19**: 289–292.

Eltner A, Schneider D. 2015. Analysis of Different Methods for 3D Reconstruction of Natural Surfaces from Parallel-Axes UAV Images. *The Photogrammetric Record* **30**(151): 279–299. DOI:10.1111/phor.12115.

Ergenzinger P, de Jong C. 2003. Perspectives on bed load measurement. In Erosion and Sediment Transport Measurement in Rivers: Technological and Methodological Advances (Proceedings of the Oslo Workshop, June 2002), IAHS Publication 283. IAHS Press: Wallingford; 113–125.

Erlingsson U. 1991. A sensor for measuring erosion and deposition. *Journal of Sedimentary Petrology* **61**(4): 620–623.

Evans R. 1967. On the use of welding rod for erosion and deposition pins. *Revue de Géomorphologie Dynamique* **17**(4): 165.

Ferguson RI. 1986. River loads underestimated by rating curves. *Water Resources Research* **22**(1): 74–76.

Finnegan NJ, Schumer R, Finnegan S. 2014. A signature of transience in bedrock river incision rates over timescales of 10^4–10^7 years. *Nature* **505**: 391–394. DOI:10.1038/nature12913.

Fischer AG. 1969. Geological time-distance rates: the Bubnoff unit. *Geological Society of America Bulletin* **80**: 549–552.

Fleming G. 1969. Suspended solids monitoring: a comparison between three instruments. *Water and Water Engineering* **72**: 377–382.

Flowers RM, Farley KA. 2012. Apatite ^{4}He/^{3}He and (U-Th)/He evidence for an ancient Grand Canyon. *Science* **338**: 1616–1619. DOI:10.1126/science.1229390.

Fonstad MA, Dietrich JT, Courville BC, Jensen JL, Carbonneau PE. 2013. Topographic structure from motion: a new development in photogrammetric measurement. *Earth Surface Processes and Landforms* **38**(4): 421–430. DOI:10.1002/esp.3366.

Gaeuman D, Holt CR, Bunte K. 2015. Maximum likelihood parameter estimation for fitting bedload rating curves. *Water Resources Research* **51**: 281–301. DOI:10.1002/2014WR015872.

Galy A, France-Lanord C. 2001. Higher erosion rates in the Himalaya: geochemical constraints on riverine fluxes. *Geology* **29**(1): 23–26.

Gardner TW, Jorgensen DW, Shuman C, Lemieux CR. 1987. Geomorphic and tectonic process rates: effects of measured time interval. *Geology* **15**: 259–261. DOI:10.1130/0091-7613(1987)15<259:GATPRE>2.0.CO;2.

Gill ED, Lang JG. 1983. Micro-erosion meter measurements of rock wear on the Otway Coast of Southeast Australia. *Marine Geology* **52**: 141–156.

Gilbert GK. 1877. Land sculpture. In *Geology of the Henry Mountains, Utah*, Hunt CB (ed.), Geological Society of America 167. The Geological Society of America: Boulder, CO; 99–150.

Gleason CH. 1957. Reconnaissance methods of measuring erosion. *Journal of Soil and Water Conservation* **12**(3): 105–107.

Gómez-Gutiérrez A, Schnabel S, Berenguer-Sempere F, Lavado-Contador F, Rubio-Delgado J. 2014. Using 3D photo- reconstruction methods to estimate gully headcut erosion. *Catena* **120**: 91–101. DOI:10.1016/j.catena.2014.04.004.

Gosse JC, Phillips FM. 2001. Terrestrial in situ cosmogenic nuclides: theory and application. *Quaternary Science Reviews* **20**: 1475–1560. DOI:10.1016/S0277-3791(00)00171-2.

Granger DE, Riebe CS. 2014. Cosmogenic nuclides in weathering and erosion. In Treatise on Geochemistry, second edition. Elsevier: Amsterdam; 402–436. DOI. 10.1016/B978-0-08-095975-7.00514-3

Granger DE, Muzikar PF. 2001. Dating sediment burial with cosmogenic nuclides: theory, techniques, and limitations. *Earth and Planetary Science Letters* **188**(1–2): 269–281. DOI:10.1016/S0012-821X(01)00236-9.

Granger DE, Kirchner JW, Finkel R. 1996. Spatially averaged long-term erosion rates measured from in situ-produced cosmogenic nuclides in alluvial sediment. *The Journal of Geology* **104**: 249–257.

Gray JR, Laronne JB, Marr JDG (eds). 2010. Bedload-surrogate Monitoring Technologies, US Geological Survey Scientific Investigations Report 2010–5091. US Geological Survey: Reston, VA. http://pubs.usgs.gov/sir/2010/5091/

Hadley RF, Lusby GC. 1967. Runoff and hillslope erosion resulting from a high-intensity thunderstorm near Mack, Western Colorado. *Water Resources Research* **3**(1): 139–143.

Haigh MJ. 1977. The use of erosion pins in the study of slope evolution. *British Geomorphological Research Group, Technical Bulletin* **18**: 31–49.

Hancock G, Kirwan M. 2007. Summit erosion rates deduced from 10Be: implications for relief production in the central Appalachians. *Geology* **35**: 89–92. DOI:10.1130/0016-7606(2002)114.

Hancock GS, Anderson RS, Whipple KX. 1998. Beyond power: bedrock river incision process and form. In Rivers over Rock: Fluvial Processes in Bedrock, Tinkler KJ, Wohl EE (eds). American Geophysical Union: Washington, DC; 35–60.

Hanna FK. 1966. A technique for measuring the rate of erosion of cave passages. *Proceedings University of Bristol Speleology Society* **11**: 83–86.

Harkins N, Kirby E, Heimsath A, Robinson R, Reiser U. 2007. Transient fluvial incision in the headwaters of the Yellow River, northeastern Tibet, China. *Journal of Geophysical Research* **112**: F03S04. DOI:10.1029/2006JF000570.

Hartshorn K, Hovius N, Dade WB, Slingerland RL. 2002. Climate-driven bedrock incision in an active mountain belt. *Science* **297**: 2036–2038. DOI:10.1126/science.1075078.

Harwin S, Lucieer A, Osborn J. 2015. The impact of the calibration method on the accuracy of point clouds derived using unmanned aerial vehicle multi-view stereopsis. *Remote Sensing* **7**(9): 11933–11953. DOI:10.3390/rs70911933.

Haschenburger JK, Church M. 1998. Bed material transport estimated from the virtual velocity of sediment. *Earth Surface Processes and Landforms* **23**(9): 791–808. DOI:10.1002/(SICI)1096-9837(199809)23:9<791::AID-ESP888>3.0.CO;2-X.

Hassan MA. 1990. Scour, fill, and burial depth of coarse material in gravel bed streams. *Earth Surface Processes and Landforms* **15**: 341–356.

Häuselmann PH, Granger D, Jeannin P-Y, Lauritzen SE. 2007. Abrupt glacial valley incision at 0.8 Ma dated from cave deposits in Switzerland. *Geology* **35**(2): 143–146. DOI:10.1130/G23094A.

Heimann FUM, Rickenmann D, Böckli M, Badoux A, Turowski JM, Kirchner JW. 2014. Calculation of bedload transport in Swiss mountain rivers using the model sedFlow: proof of concept. *Earth Surface Dynamics* **3**: 15–34. DOI:10.5194/esurf-3-15-2015.

Heimsath AM. 2006. Eroding the land: steady-state and stochastic rates and processes through a cosmogenic lens. *GSA Special Paper* **415**: 111–129. DOI:10.1130/2006.2415(07).

Heimsath AM, Farid H. 2002. Hillslope topography from unconstrained photographs. *Mathematical Geology* **34**(8): 929–952. DOI:10.1023/A:1021364623017.

Heimsath AM, Dietrich WE, Nishiizumi K, Finkel RC. 1997. The soil production function and landscape equilibrium. *Nature* **388**: 358–361.

Helley EJ, Smith W. 1971. Development and Calibration of a Pressure-difference Bedload Sampler. US Department of the Interior, Geological Survey, Water Resources Division: Menlo Park, CA; 18.

Heritage G, Hetherington D. 2007. Towards a protocol for laser scanning in fluvial geomorphology. *Earth Surface Processes and Landforms* **32**: 66–74. DOI:10.1002/esp.1375.

Herman F, Rhodes E, Braun J, Heiniger L. 2010. Uniform erosion rates and relief amplitude during glacial cycles in the Southern Alps of New Zealand, as revealed from OSL–thermochronology. *Earth and Planetary Science Letters* **297**: 183–189. DOI:10.1016/j.epsl.2010.06.019.

Herman F, Seward D, Valla PG, Carter A, Kohn B, Willett SD, Ehlers TA. 2013. Worldwide acceleration of mountain erosion under a cooling climate. *Nature* **504**: 423–426. DOI:10.1038/nature12877.

High CJ, Hanna FK. 1970. A method for the direct measurement of erosion on rock surfaces. *British Geomorphological Research Group Technical Bulletin* **5**: 1–25.

Hilldale RC, Raff D. 2007. Assessing the ability of airborne lidar to map river bathymetry. *Earth Surface Processes and Landforms* **33**: 773–783. DOI:10.1002/esp.1575.

Hirschi MC, Barfield BJ, Moore ID, Colliver DG. 1987. Profile meters for detailed measurement of soil surface heights. *Applied Engineering in Agriculture* **3**: 47–51.

Hodge R, Brasington J, Richards K. 2009. In situ characterization of grain-scale fluvial morphology using terrestrial laser scanning. *Earth Surface Processes and Landforms* **34**: 954–968. DOI:10.1002/esp.1780.

Holtschlag DJ. 2001. Optimal estimation of suspended-sediment concentrations in streams. *Hydrological Processes* **15**: 1133–1155. DOI:10.1002/hyp.207.

House M, Wernicke BP, Farley KA. 1998. Dating topography of the Sierra Nevada, California, using apatite (U–Th)/He ages. *Nature* **396**: 66–69.

Hovius N, Stark CP, Allen PA. 1997. Sediment flux from a mountain belt derived by landslide mapping. *Geology* **25**(3): 231–234.

Hovius N, Meunier P, Lin CW, Chen H, Chen YG, Dadson S, Horng MJ, Lines M. 2011. Prolonged seismically induced erosion and the mass balance of a large earthquake. *Earth and Planetary Science Letters* **304**: 347–355. DOI:10.1016/j.epsl.2011.02.005.

Howard AD, Kerby G. 1983. Channel changes in badlands. *Geological Society of America Bulletin* **94**: 739–752.

Hudson NW. 1964. Field measurements of accelerated soil erosion in localized areas. *Rhodesia Agricultural Journal* **31**(3): 46–48.

Imeson AC. 1971. Heather burning and soil erosion on the North Yorkshire Moors. *Journal of Applied Ecology* **8**(2): 537–542.

Ivy-Ochs S, Poschinger AV, Synal H-A, Maisch M. 2009. Surface exposure dating of the Flims landslide, Graubünden, Switzerland. *Geomorphology* **103**(1): 104–112. DOI:10.1016/j.geomorph.2007.10.024.

James MR, Robson S. 2012. Straightforward reconstruction of 3D surfaces and topography with a camera: accuracy and geoscience application. *Journal of Geophysical Research* **117** . DOI:10.1029/2011jf002289.F03017

James MR, Robson S. 2014. Mitigating systematic error in topographic models derived from UAV and ground-based image networks. *Earth Surface Processes and Landforms* **39**(10): 1413–1420. DOI:10.1002/esp.3609.

Johnson JPL, Whipple KX, Sklar LS. 2010. Contrasting bedrock incision rates from snowmelt and flash floods in the Henry Mountains, Utah. *Geological Society of America Bulletin* **122**: 1600–1615. DOI:10.1130/B30126.1.

Karlstrom KE, Crow RS, Peters L, McIntosh W, Raucci J, Crossey LJ, Umhoefer P, Dunbar N. 2007. 40Ar/39Ar and field studies of Quaternary basalts in Grand Canyon and model for carving Grand Canyon: quantifying the interaction of river incision and normal faulting across the western edge of the Colorado Plateau. *Geological Society of America Bulletin* **119**(11/12): 1283–1312 .DOI. 10.1130B26154.1

Khorashahi J, Byler RK, Dillaha TA. 1987. An opto-electronic soil profile meter. *Computers and Electronics in Agriculture* **2**: 145–155.

Kirchner JW, Finkel RC, Riebe CS, Granger DE, Clayton JL, King JG, Megahan WF. 2001. Mountain erosion over 10yr, 10k.y., and m.y. time scales. *Geology* **29**(7): 591–594.

Kolb A, Barth E, Koch R, Larsen R. 2010. Time-of-flight cameras in computer graphics. *Computer Graphics Forum* **29**(1): 141–159. DOI:10.1111/j.1467-8659.2009.01583.x.

Koppes MN, Montgomery DR. 2009. The relative efficacy of fluvial and glacial erosion over modern to orogenic timescales. *Nature Geoscience* **2**: 644–647. DOI:10.1038/NGEO616.

Kornecki TS, Fouss JL, Prior SA. 2008. A portable device to measure soil erosion/deposition in quarter-drains. *Soil Use and Management* **24**: 401–408. DOI:10.1111/j.1475-2743.2008.00181.x.

Ku HH. 1966. Notes on the use of propagation of error formulas. *Journal of Research of the National Bureau of Standards (National Bureau of Standards)* **70C**(4): 263–273. DOI:10.6028/jres.070c.025.

Lague D, Brodu N, Leroux J. 2013. Accurate 3D comparison of complex topography with terrestrial laser scanner: Application to the Rangitikei canyon (N-Z). *ISPRS Journal of Photogrammetry and Remote Sensing* **82**: 10–26. DOI:10.1016/j.isprsjprs.2013.04.009.

Lal D. 1991. Cosmic ray labeling of erosion surface: in-situ nuclide production rates and erosion models. *Earth and Planetary Science Letters* **161**: 231–241.

Lal D, Peters B. 1967. Cosmic ray produced radioactivity on the earth. In Handbuch der Physik, Flugge S (ed.). *Springer-Verlag: Berlin; volume* **46**: 551–612.

Lamb MP, Fonstad MA. 2010. Rapid formation of a modern bedrock canyon by a single flood event. *Nature Geoscience* **3**: 477–481. DOI:10.1038/NGEO894.

Lana-Renault N, Regüés D. 2007. Bedload transport under different flow conditions in a human-disturbed catchment in the Central Spanish Pyrenees. *Catena* **71**: 155–163. DOI:10.1016/j.catena.2006.04.029.

Lane SN, Richards KS, Chandler JH. 1995. Morphological estimation of the time-integrated bed-load transport rate. *Water Resources Research* **31**: 761–772. DOI:10.1029/94WR01726.

Lange R, Seitz P. 2001. Solid-state, time-of-flight range camera. *IEEE Journal of Quantum Electronics* **37**(3): 390–397. DOI:10.1109/3.910448.

Laronne JB, Duncan MJ. 1989. Constraints on duration of sediment storage in a wide, gravel-bed river, New Zealand. In *Sediment and*

the Environment (Proceeding of the Baltimore Symposium, May 1989), IAHS Publication 184. IAHS Press: Wallingford; 165–172.

Laronne JB, Outhet DN, Carling PA, McCabe TJ. 1994. Scour chain employment in gravel bed rivers. *Catena* **22**: 299–306.

Larsen IJ, Montgomery DR, Korup O. 2010. Landslide erosion controlled by hillslope material. *Nature Geoscience* **3**: 247–251. DOI:10.1038/ngeo776.

Lauffer H, Sommer N. 1982. Studies on sediment transport in mountain streams of the Eastern Alps. *Proceedings, 14th International Congress on Dams*, Rio de Janeiro; 431–453.

Lavé J, Dubille M. 2011. Real-time measurements and modelling of bedrock river erosion along two rivers of the Frontal Himalaya. *Geophysical Research Abstracts* **13**: EGU2011–EGU8108.

Lawler DM. 1991. A new technique for the automatic monitoring of erosion and deposition rates. *Water Resources Research* **27**(8): 2125–2128.

Lawler DM. 1992. Design and installation of a novel automatic erosion monitoring system. *Earth Surface Processes and Landforms* **17**: 455–463.

Lawler DM. 1993. The measurement of river bank erosion and lateral channel change: a review. *Earth Surface Processes and Landforms* **18**: 777–821.

Lawler DM. 2005. Defining the moment of erosion: the principle of thermal consonance timing. *Earth Surface Processes and Landforms* **30**: 1597–1615. DOI:10.1002/esp.1234.

Lawler DM. 2008. Advances in the continuous monitoring of erosion and deposition dynamics: Developments and applications of the new PEEP-3T system. *Geomorphology* **93**: 17–39. DOI:10.1016/j.geomorph.2006.12.016.

Lawler DM, West JR, Couperthwaite JS, Mitchell SB. 2001. Application of a novel automatic erosion and deposition monitoring system at a channel bank site on the tidal river Trent, U.K. *Estuarine. Coastal and Shelf Science* **53**: 237–247. DOI:10.1006/ecss.2001.0779.

Lehre AK, Collins BD, Dunne T. 1983. Post-eruption sediment budget for the North Fork Toutle River Drainage, June 1980–June 1981. *Zeitschrift für Geomorphologie, Neue Folge, Supplement Band* **46**: 143–163.

Lenzi MA, Marchi L, Scussel GR. 1990. Measurement of Coarse Sediment Transport in a Small Alpine Stream, IAHS Publication 193. IAHS Press: Wallingford; 283–290.

Leopold LB, Emmett WW, Myrick RM. 1966. *Channel and Hillslope Process in a Semiarid Area, New Mexico*, Geological Survey Professional Paper 352-G. United States Government Printing Office: Washington DC.

Li JJ, Fang XM, Van Der Voo R, Zhu JJ, MacNiocaill CM, Ono Y, Pan BT, Zhong W, Wang JL, Sasaki T, Zhang YT, Cao JX, Kang SC, Wang JM. 1997. Magnetostratigraphic dating of river terraces: Rapid and intermittent incision by the Yellow River of the northeastern margin of the Tibetan Plateau during the Quaternary. *Journal of Geophysical Research* **102**(B5): 10121–10132.

Li G, West AJ, Densmore AL, Jin Z, Parker RN, Hilton RG. 2014. Seismic mountain building: Landslides associated with the 2008 Wenchuan earthquake in the context of a generalized model for earthquake volume balance. *Geochemistry, Geophysics, Geosystems* **15**: 833–844. DOI:10.1002/2013GC005067.

Libby WF. 1955. Radiocarbon Dating. University of Chicago Press: Chicago, IL.

Lisle TE, Eads RE. 1991. *Methods to Measure Sedimentation of Spawning Gravels*, USDA Forest Service Research Note PSW-411. USDA: Washington, DC.

Lowe JJ (ed.). 1991. Radiocarbon dating: recent applications and future potential. *Quaternary Proceedings* **1**: 1–89.

Lowe DJ. 2011. Tephrochronology and its application: a review. *Quaternary Geochronology* **6**: 107–153. DOI:10.1016/j.quageo.2010.08.003.

Lucía A, Laronne JB, Martín-Duque JF. 2011. Geodynamics processes on sandy slope gullies in central Spain: field observations, methods and measurements in a singular system. *Geodinamica Acta* **24**(2): 61–79. DOI:10.3166/ga.24.61-79.

Lupker M, Blard PH, Lavé J, France-Lanord C, Leanni L, Puchol N, Charreau J, Bourlès D. 2012. ^{10}Be-derived Himalayan denudation rates and sediment budgets in the Ganga basin. *Earth and Planetary Science Letters* **333–334**: 146–156. DOI:10.1016/j.epsl.2012.04.020.

Madsen AT, Murray AS. 2009. Optically stimulated luminescence dating of young sediments: a review. *Geomorphology* **109**: 3–16. DOI:10.1016/j.geomorph.2008.08.020.

Malamud BD, Turcotte DL, Guzzetti F, Reichenbach P. 2004. Landslide inventories and their statistical properties. *Earth Surface Processes and Landforms* **29**: 687–711. DOI:10.1002/esp.1064.

Mao L, Dell'Agnese A, Huincache C, Penna D, Engel M, Niedrist G, Comiti F. 2014. Bedload hysteresis in a glacier-fed mountain river. *Earth Surface Processes and Landforms* **39**: 964–976. DOI:10.1002/esp.3563.

Marc O, Hovius N. 2015. Amalgamation in landslide maps: effects and automatic detection. *Natural Hazards and Earth System Sciences* **15**: 723–733. DOI:10.5194/nhess-15-723-2015.

Marc O, Hovius N, Meunier P, Gorum T, Uchida T. 2016. A seismologically consistent expression for the total area and volume of earthquake-triggered landsliding. *Journal of Geophysical Research* **121**: 640–663. DOI:10.1002/2015JF003732.

Mark DM, Church M. 1977. On the misuse of regression Earth Science. *Mathematical Geology* **9**(1): 63–75.

McCool DK, Dossett MG, Yecha SJ. 2013. A portable rill meter for field measurement of soil loss, Erosion and Sediment Transport Measurement (Proceedings of the Florence Symposium, June 1981). IAHS Publ. no. 133. p. 479–484.

McKean J, Nagel D, Tonina D, Bailey P, Wright CW, Bohn C, Nayegandhi A. 2009. Remote sensing of channels and riparian zones with a narrow-beam aquatic-terrestrial lidar. *Remote Sensing* **1**(4): 1065–1096. DOI:10.3390/rs1041065.

Meunier P, Métivier F, Lajeunesse E, Mériaux AS, Faure J. 2006. Flow pattern and sediment transport in a braided river: the "torrent de St Pierre" (French Alps). *Journal of Hydrology* **330**: 496–505. DOI:10.1016/j.jhydrol.2006.04.009.

Miller DM. 1984. Reducing transformation bias in curve fitting. *The American Statistician* **38**(2): 124–126.

Miller JP, Leopold LB. 1962. Simple measurements of morphological changes in river channels and hill slopes. *Arid Zone Research* **20**: 421–427.

Molnar P, Anderson RS, Kier G, Rose J. 2006. Relationships among probability distributions of stream discharges in floods, climate, bed load transport, and river incision. *Journal of Geophysical Research* **111** . DOI:10.1029/2005JF000310.F02001

Montgomery DR. 2004. Observations on the role of lithology in strath terrace formation and bedrock channel width. *American Journal of Science* **304**: 454–476. DOI:10.2475/ajs.304.5.454.

Nagihara S, Mulligan KR, Xiong W. 2004. Use of a three-dimensional laser scanner to digitally capture the topography of sand dunes in high spatial resolution. *Earth Surface Processes and Landforms* **29**: 391–398. DOI:10.1002/esp.1026.

Nawa RK, Frissell CA. 1993. Measuring scour and fill of gravel streambeds with scour chains and sliding-bead monitors. *North American Journal of Fisheries Management* **13**: 634–639.

Nex F, Gerke M, Remondino F, Przybilla HJ, Bäumker M, Zurhorst A. 2015. ISPRS benchmark for multi-platform photogrammetry. *ISPRS Annals of the Photogrammetry. Remote Sensing and Spatial Information Sciences* **II-3**(W4): 135–142. DOI:10.5194/isprsannals-II-3-W4-135-2015.

Niemi N, Oskin M, Burbank D, Heimsath A, Gabet E. 2005. Effects of bedrock landslides on cosmogenically determined erosion rates. *Earth and Planetary Science Letters* **237**: 480–498. DOI:10.1016/j.epsl.2005.07.009.

Nishiizumi K, Winterer EL, Kohl CP, Klein J, Middleton R, Lal D, Arnold JR. 1989. Cosmic ray production rates of ^{10}Be and ^{26}Al in quartz from glacially polished rocks. *Journal of Geophysical Research* **94**(B12): 17907–17915. DOI:10.1029/JB094iB12p17907.

Nitsche M, Turowski JM, Badoux A, Pauli M, Schneider J, Rickenmann D, Kohoutek TK. 2010. Measuring streambed morphology using range imaging. In River Flow 2010, Dittrich A, Koll K, Aberle J, Geisenhainer P (eds). Bundesamt für Wasserbau: Braunschweig; 1715–1722.

Nitsche M, Rickenmann D, Turowski JM, Badoux A, Kirchner JW. 2011. Evaluation of bedload transport predictions using flow resistance equations to account for macro-roughness in steep mountain streams. *Water Resources Research* **47**: W08513. DOI:10.1029/2011WR010645.

Nitsche M, Turowski JM, Badoux A, Rickenmann D, Kohoutek TK, Pauli M, Kirchner JW. 2013. Range imaging: A new method for high-resolution topographic measurements in small- and medium-scale field sites. *Earth Surface Processes and Landforms* **38**: 810–825. DOI:10.1002/esp.3322.

Northend CA. 1967. Lidar, a laser radar for meteorological studies. *Die Naturwissenschaften* **54**(4): 77–80.

Hudson NW. 1993. Field Measurement of Soil Erosion and Runoff. Silsoe Associates: Ampthill.

Ojala AEK, Francus P, Zolitschka B, Besonen M, Lamoureux SF. 2012. Characteristics of sedimentary varve chronologies – A review. *Quaternary Science Reviews* **43**: 45–60. DOI:10.1016/j.quascirev.2012.04.006.

Okoba BO, Sterk G. 2006. Farmers' identification of erosion indicators and related erosion damage in the Central Highlands of Kenya. *Catena* **65**: 292–301. DOI:10.1016/j.catena.2005.12.004.

Pederson J, Karlstrom K, Sharp W, McIntosh W. 2002. Differential incision of the Grand Canyon related to Quaternary faulting –Constraints from U-series and Ar/Ar dating. *Geology* **30**: 739–742. DOI:10.1130/0091-7613-31.1.e16.

Polyak V, Hill C, Asmerom Y. 2008. Age and evolution of the Grand Canyon revealed by U-Pb dating of water table–type speleothems. *Science* **319**: 1377–1380. DOI:10.1126/science.1151248.

Poppe LJ, Ackerman SD, Doran EF, Beaver AL, Crocker JM, Schattgen PT. 2006. *Interpolation of Reconnaissance Multibeam Bathymetry from North-central Long Island Sound*, Open File Report 2005-1145, US Geological Society. http://woodshole.er.usgs.gov/pubs/of2005-1145/index.html [July 2016].

Portenga EW, Bierman PR. 2011. Understanding Earth's eroding surface with ^{10}Be. *Geological Society of America Today* **21**: 4–10. DOI:10.1130/G111A.1.

Pratt-Sitaula B, Garde M, Burbank DW, Oskin M, Heimsath A, Gabet E. 2007. Bedload-to-suspended load ratio and rapid bedrock incision from Himalayan landslide-dam lake record. *Quatern. Res.* **68**: 111–120. DOI:10.1016/j.yqres.2007.03.005.

Prince PS, Spotila JA. 2013. Evidence of transient topographic disequilibrium in a landward passive margin river system: knickpoints and paleolandscapes of the New River basin, southern Appalachians. *Earth Surface Processes and Landforms* **38**: 1685–1699. DOI:10.1002/esp.3406.

Rahl JM, Ehlers TA, van der Pluijm BA. 2007. Quantifying transient erosion of orogens with detrital thermochronology from syntectonic basin deposits. *Earth and Planetary Science Letters* **256**: 147–161. DOI:10.1016/j.epsl.2007.01.020.

Rapp A, Murray-Rust DH, Christiansson C, Berry L. 1972. Soil erosion and sedimentation in four catchments near Dodoma, Tanzania. *Geografiska Annaler* **54A**(3–4): 255–318.

Rasmussen PP, Gray JR, Glysson GD, Ziegler AC. 2009. *Guidelines and Procedures for Computing Time-series Suspended-sediment Concentrations and Loads from In-stream Turbidity-sensor and Streamflow data*, US Geological Survey Techniques and Methods Book 3, Chapter C4. US Geological Survey: Reston, VA; 53 pp.

Reid I, Layman JT, Frostick LE. 1980. The continuous measurement of bedload discharge. *Journal of Hydraulic Research* **18**(3): 243–249. DOI:10.1080/00221688009499550.

Reid I, Bathurst JC, Carling PA, Walling DE, Webb BW. 1997. Sediment erosion, transport and deposition. In Applied Fluvial Geomorphology for River Engineering and Management, Thorne CR, Hey RD, Newson MD (eds). John Wiley & Sons: Chichester; 95–135.

Reiners PW, Brandon MT. 2006. Using thermochronology to understand orogenic erosion. *Annual Review of Earth and Planetary Sciences* **34**: 419–466. DOI:10.1146/annurev.earth.34.031405.125202.

Repka JL, Anderson RS, Finkel RC. 1997. Cosmogenic dating of fluvial terraces, Fremont River, Utah. *Earth and Planetary Science Letters* **152**: 59–73. DOI:10.1016/S0012-821X(97)00149-0.

Reusser L, Bierman P, Pavich M, Larsen J, Finkel R. 2006. An episode of rapid bedrock channel incision during the last glacial cycle, measured with 10Be. *American Journal of Science* **306**: 69–102. DOI:10.2475/ajs.306.2.69.

Rickenmann D. 2015. Bedload transport measurements with geophones, hydrophones, and underwater microphones (passive acoustic methods). *Proceedings of Gravel Bed Rivers 8: Gravel Bed Rivers and Disasters*, Kyoto/Takayam, September 2015.

Rickenmann D, McArdell BW. 2008. Calibration of piezoelectric bedload impact sensors in the Pitzbach mountain stream. *Geodynamica Acta* **21**: 35–52. DOI:10.3166/ga.21.35-52.

Rickenmann D, Turowski JM, Fritschi B, Klaiber A, Ludwig A. 2012. Bedload transport measurements at the Erlenbach stream with geophones and automated basket samplers. *Earth Surface Processes and Landforms* **37**: 1000–1011. DOI:10.1002/esp.3225.

Rickenmann D, Turowski JM, Fritschi B, Wyss C, Laronne J, Barzilai R, Reid I, Kreisler A, Aigner J, Seitz H, Habersack H. 2014. Bedload transport measurements with impact plate geophones: comparison of sensor calibration in different gravel-bed streams. *Earth Surface Processes and Landforms* **39**: 928–942. DOI:10.1002/esp.3499.

Rieke-Zapp DH. 2010. A digital medium-format camera for metric applications – ALPA 12 METRIC. *The Photogrammetric Record* **25** (131): 283–298. DOI:10.1111/j.1477-9730.2010.00586.x.

Ring J. 1963. The laser in astronomy. *The New Scientist June* **20**: 672–673.

Robinson LA. 1976. The micro-erosion meter technique in a littoral environment. *Marine Geology* **22**: M51–M58.

Römkens MJM, Singarayar S, Gantzer CJ. 1986. An automated non-contact surface profile meter. *Soil & Tillage Research* **6**: 193–202.

Sadler PM. 1981. Sediment accumulation rates and the completeness of stratigraphic sections. *Journal of Geology* **89**: 569–584.

Sadler PM. 1999. The influence of hiatuses on sediment accumulation rates. In *GeoResearch Forum* 5, Bruns P, Haas HC (eds). Trans Tech Publications: Pfaffikon; 15–40.

Sasowsky ID, White WB, Schmidt VA. 1995. Determination of stream-incision rate in the Appalachian plateaus by using cave-sediment magnetostratigraphy. *Geology* **23**: 415–418.

Schaefer M, Inkpen R. 2010. Towards a protocol for laser scanning of rock surfaces. *Earth Surface Processes and Landforms* **35**: 417–423. DOI:10.1002/esp.1938.

Schaller M, Hovius N, Willett SD, Ivy-Ochs S, Synal HA, Chen MC. 2005. Fluvial bedrock incision in the active mountain belt of Taiwan from in situ-produced cosmogenic nuclides. *Earth Surface Processes and Landforms* **30**(8): 955–971. DOI:10.1002/esp.1256.

Schildgen TF, Hodges KV, Whipple KX, Reiners PW, Pringle MS. 2007. Uplift of the western margin of the Andean plateau revealed from canyon incision history, southern Peru. *Geology* **35**(6): 523–526. DOI:10.1130/G23532A.1.

Schildgen TF, Cosentino D, Bookhagen B, Niedermann S, Yildirim C, Echtler HP, Wittmann H, Strecker MR. 2012. Multi-phase uplift of the southern margin of the Central Anatolian plateau: a record of tectonic and upper mantle processes. *Earth and Planetary Science Letters* **317–318**: 85–95. DOI:10.1016/j.epsl.2011.12.003.

Schleppi P, Waldner PA, Fritschi B. 2006. Accuracy and precision of different sampling strategies and flux integration methods for runoff water: comparisons based on measurements of the electrical conductivity. *Hydrological Processes* **20**: 395–410. DOI:10.1002/hyp.6057.

Schmid T, Schack-Kirchner H, Hildebrand E. 2004. A case study of terrestrial laser-scanning in erosion research: calculation of roughness indices and volume balance at a logged forest site. *International Archives of Photogrammetry, Remote Sensing and Spatial Information Sciences* 36(8/W2): 114–118.

Schneider JM, Turowski JM, Rickenmann D, Hegglin R, Arrigo S, Mao L, Kirchner JW. 2014. Scaling relationships between bed load volumes, transport distances, and stream power in steep mountain channels. *Journal of Geophysical Research* **119**: 533–549. DOI:10.1002/2013JF002874.

Schneider JM, Rickenmann D, Turowski JM, Bunte K, Kirchner JW. 2015. Applicability of bedload transport models for mixed size sediments in steep streams considering macro-roughness. *Water Resources Research* **51**(7): 5260–5283. DOI:10.1002/2014WR016417.

Schuett-Hames D, Conrad B, Pleus A, Lautz K. 1996. *Literature Review & Monitoring Recommendations for Salmonid Spawning Gravel Scour*, Technical report, TFW Ambient Monitoring Program, TFW-AM-9-96-001. NWIFC: Olympia, WA.

Schumer R, Jerolmack DJ. 2009. Real and apparent changes in sediment deposition rates through time. *Journal of Geophysical Research* 114: F00A06. DOI. 10.1029/2009JF001266

Schwarcz HP. 1989. Uranium series dating of Quaternary deposits. *Quaternary International* **1**: 7–17.

Sharp WD, Ludwig KR, Chadwick OA, Amundson R, Glaser LL. 2003. Dating fluvial terraces by Th-230/U on pedogenic carbonate, Wind River Basin, Wyoming. *Quaternary Research* **59**: 139–150. DOI. 10.1016/S0033–5894(03)00003–6.

Shuster DL, Ehlers TA, Rusmore ME, Farley KA. 2005. Rapid glacial erosion at 1.8 Ma revealed by ^{4}He/^{3}He thermochronometry. *Science* **310**: 1668–1670. DOI:10.1126/science.1118519.

Smart G, Aberle J, Duncan M, Walsh J. 2004. Measurement and analysis of alluvial bed roughness. *Journal of Hydraulic Research* **42**(3): 227–237. DOI:10.1080/00221686.2004.9641191.

Spate AP, Jennings JN, Smith DI, Greenaway MA. 1985. The micro-erosion meter: use and limitations. *Earth Surface Processes and Landforms* **10**: 427–440.

Spencer T. 1981. Micro-topographic change on calcarenites, Grand Cayman Island, West Indies. *Earth Surface Processes and Landforms* **6**: 85–94.

Squires GL. 1998. *Practical Physics*, reprint of the third edition. Cambridge University Press: Cambridge.

Stark CP, Hovius N. 2001. The characterization of landslide size distribution. *Geophysical Research Letters* **28**(6): 1091–1094. DOI:10.1029/2000GL008527.

Stephenson WJ. 1997. Improving the traversing micro-erosion meter. *Journal of Coastal Research* **13**(1): 236–241.

Stephenson W. 2013. The micro and traversing erosion meter. In Treatise on Geomorphology, Shroder J (Editor-in-Chief), Kennedy D, Switzer AD (eds). Academic Press: San Diego, CA; volume **14**, 164–169.

Stephenson WJ, Finlayson BL. 2009. Measuring erosion with the micro-erosion meter – contributions to understanding landform evolution. *Earth-Science Reviews* **95**: 53–62. DOI:10.1016/j.earscirev.2009.03.006.

Stephenson WJ, Kirk RM. 1998. Rates and patterns of erosion on intertidal shore platforms, Kaikoura Peninsula, South Island, New Zealand. *Earth Surface Processes and Landforms* **23**: 1071–1085.

Stephenson WJ, Kirk RM, Kennedy DM, Finlayson BL, Chen Z. 2012. Long term shore platform surface lowering rates: revisiting Gill and Land after 32 years. *Marine Geology* **299–300**: 90–95. DOI:10.1016/j.margeo.2012.01.005.

Stock GM, Granger DE, Sasowsky ID, Anderson RC. 2005. Comparison of U-Th, paleomagnetism, and cosmogenic burial methods for dating caves: implications for landscape evolution studies. *Earth and Planetary Science Letters* **326**: 388–403. DOI:10.1016/j.epsl.2005.04.024.

Stock JD, Montgomery DR, Collins BD, Dietrich WE, Sklar L. 2005. Field measurements of incision rates following bedrock exposure: Implications for process controls on the long profiles of valleys cut by rivers and debris flows. *Geological Society of America Bulletin* **117**(11/12): 174–194. DOI:10.1130/B25560.1.

Stoffel M, Corona C, Ballersteros-Cánovas JA, Bodoque JM. 2013. Dating and quantification of erosion processes based on exposed roots. *Earth-Science Reviews* **123**: 18–34. DOI:10.1016/j.earscirev.2013.04.002.

Surian N, Mao L, Giacomin M, Ziliani L. 2009. Morphological effects of different channel-forming discharges in a gravel-bed river. *Earth Surface Processes and Landforms* **34**: 1093–1107. DOI:10.1002/esp.1798.

Swantesson JOH, Moses CA, Berg GE, Jansson KM. 2006. Methods for measuring shore platform micro erosion: a comparison of the micro-erosion meter and laser scanner. *Zeitschrift für Geomorphologie, Neue Folge, Supplement Band* **144**: 1–17.

Trinder JC, Jansa J, Huang Y. 1995. An assessment of the precision and accuracy of methods of digital target location. *ISPRS Journal of Photogrammetry and Remote Sensing* **50**(2): 12–20.

Trudgill S. 1977. Problems in the estimation of short-term variations in limestone erosion processes. *Earth Surface Processes* **2**: 251–256.

Trudgill S, High CJ, Hanna FK. 1981. Improvements to the micro-erosion meter. *British Geomorphological Research Group, Technical Bulletin* **29**: 3–17.

Turowski JM, Hovius N, Hsieh ML, Lague D, Chen MC. 2008. Distribution of erosion across bedrock channels. *Earth Surface Processes and Landforms* **33**: 353–363. DOI:10.1002/esp.1559.

Turowski JM, Yager EM, Badoux A, Rickenmann D, Molnar P. 2009. The impact of exceptional events on erosion, bedload transport and channel stability in a step-pool channel. *Earth Surface Processes and Landforms* **34**: 1661–1673. DOI:10.1002/esp.1855.

Turowski JM, Rickenmann D, Dadson SJ. 2010. The partitioning of the total sediment load of a river into suspended load and bedload: a review of empirical data. *Sedimentology* **57**: 1126–1146. DOI:10.1111/j.1365-3091.2009.01140.x.

Turowski JM, Badoux A, Leuzinger J, Hegglin R. 2013. Large floods, alluvial overprint, and bedrock erosion. *Earth Surface Processes and Landforms* **38**: 947–958. DOI:10.1002/esp.3341.

Valla PG, van der Beek PA, Shuster DL, Braun J, Herman F, Tassan-Got L, Gautheron C. 2012. Late Neogene exhumation and relief development of the Aar and Aiguilles Rouges massifs (Swiss Alps) from low-temperature thermochronology modeling and $^{4}He/^{3}He$ thermochronometry. *Journal of Geophysical Research* **117** . DOI:10.1029/2011JF002043.F01004

Vanmaercke M, Poesen J, Verstraeten G, de Vente J, Ocakoglu F. 2011. Sediment yield in Europe: Spatial patterns and scale dependency. *Geomorphology* **130**: 142–161. DOI:10.1016/j.geomorph.2011.03.010.

Vann Jones (née Norman) EC, Rosser NJ, Brain MJ, Petley DN. 2015. Quantifying the environmental controls on erosion of a hard rock cliff. *Marine Geology* **363**: 230–242. DOI:10.1016/j.margeo.2014.12.008.

Vanoni VA (ed.). 1975. Sedimentation Engineering. American Society of Civil Engineers: New York.

Vanwalleghem T, Laguna A, Giráldez JV, Jiménez-Hornero FJ. 2010. Applying a simple methodology to assess historical soil erosion in olive orchards. *Geomorphology* **114**: 294–302. DOI:10.1016/j.geomorph.2009.07.010.

Walker MJC. 2005. Quaternary Dating Methods. John Wiley & Sons: Chichester.

Walling DE, Webb BW. 1981. The reliability of suspended sediment load data. In Erosion and Sediment Transport Measurement (Proceedings of the Florence Symposium, June 1981), IAHS Publication 133. IAHS Press: Wallingford; 177–194.

Walling DE, Webb BW. 1987. Suspended load in gravel-bed rivers: UK experience. In Sediment Transport in Gravel-bed Rivers, Thorne CR, Bathurst JC, Hey RD (eds). John Wiley & Sons: Chichester; 691–732.

Wallinga J. 2002. Optically stimulated luminescence dating of fluvial deposits: a review. *Boreas* **31**: 303–322. DOI:10.1111/j.1502-3885.2002.tb01076.x.

Westoby MJ, Brasington J, Glasser NF, Hambrey MJ, Reynolds JM. 2012. 'Structure-from-Motion' photogrammetry a low-cost, effective tool for geoscience applications. *Geomorphology* **179**: 300–314. DOI:10.1016/j.geomorph.2012.08.021.

Whipple KX, Snyder NP, Dollenmayer K. 2000. Rates and processes of bedrock incision by the upper Ukak River since the 1912 Novarupta ash flow in the Valley of Ten Thousand Smokes, Alaska. *Geology* **28**: 835–838. DOI:10.1130/0091-7613(2000)28<835:RAPOBI>2.0.CO;2.

Willenbring JK, von Blanckenburg F. 2010a. Long-term stability of global erosion rates and weathering during late-Cenozoic cooling. *Nature* **465**: 211–214. DOI:10.1038/nature09044.

Willenbring JK, von Blanckenburg F. 2010b. Meteoric cosmogenic beryllium-10 adsorbed to river sediment and soil: applications for Earth-surface dynamics. *Earth-Science Reviews* **98**: 105–122. DOI:10.1016/j.earscirev.2009.10.008.

Williams RBG, Swantesson JOH, Robinson DA. 2000. Measuring rates of surface downwearing and mapping microtopography: the use of micro-erosion meters and laser scanner in rock weathering studies. *Zeitschrift für Geomorphologie, Neue Folge, Supplement-Band* **120**: 51–66.

Wilson A, Hovius N, Turowski JM. 2013. Upstream-facing convex surfaces: bedrock bedforms produced by fluvial bedload abrasion. *Geomorphology* **180–181**: 187–204. DOI:10.1016/j.geomorph.2012.10.010.

Yager EM, Turowski JM, Rickenmann D, McArdell BW. 2012. Sediment supply, grain protrusion, and bedload transport in mountain streams. *Geophysical Research Letters* **39** . DOI:10.1029/2012GL051654. L10402

Yanites BJ, Tucker GE, Mueller KJ, Chen YG, Wilcox T, Huang SY, Shi KW. 2010. Incision and channel morphology across active structures along the Peikang River, central Taiwan: implications for the importance of channel width. *Geological Society of America Bulletin* **122**: 1192–1208. DOI:10.1130/B30035.1.

Zentmyer R, Myrow PM, Newell DL. 2008. Travertine deposits from along the South Tibetan Fault System near Nyalam, Tibet. *Geological Magazine* **145**: 753–765. DOI:10.1017/S0016756808005323.

Zolitschka B. 2003. Dating based on freshwater and marine laminated sediments. In Global Change in the Holocene, Mackay A, Battarbee R, Birks J, Oldfield F (eds). Edward Arnold Publishers: London; 92–106.

